CR 134705

CONTRACT NUMBER
NAS3-19760

SCREENING OF REDOX COUPLES AND ELECTRODE MATERIALS

Division of Energy Storage Systems

Electric Power and Storage Division

FINAL REPORT

By:

J. Giner

L. Swette

K. Cahill

GINER, INC.
14 Spring Street
Waltham, Massachusetts 02154

September, 1976

Prepared for:

NASA – Lewis Research Center
21000 Brookpark Road
Cleveland, Ohio 44154

CR 134705

CONTRACT NUMBER
NAS3-19760

SCREENING OF REDOX COUPLES AND ELECTRODE MATERIALS

FINAL REPORT

By:

J. Giner

L. Swette

K. Cahill

GINER, INC.
14 Spring Street
Waltham, Massachusetts 02154

September, 1976

Prepared for:

NASA - Lewis Research Center
21000 Brookpark Road
Cleveland, Ohio 44154

TABLE OF CONTENTS

ABSTRACT

The overall objective of this program was to measure electrochemical parameters of selected redox couples that might be potentially promising for application in bulk energy storage systems. This was carried out in two phases: a broad investigation of the basic characteristics and behavior of various redox couples followed by a more limited investigation of their electrochemical performance in a redox flow reactor configuration.

The primary objective of the first phase of the program was to evaluate eight redox couples under a variety of conditions in terms of their exchange current densities as measured by the rotating disk electrode procedure. The redox couples investigated in this first phase were: Fe^{+2}/Fe^{+3}, Ti^{+3}/Ti^{IV}, Cr^{+2}/Cr^{+3}, Sn^{+2}/Sn^{+4}, Br^{-}/Br_3^{-}, Sb^{+3}/Sb^{+5}, $Cu(NH_3)_2^{+1}/Cu(NH_3)_4^{+2}$, and $Cr(CN)_6^{-4}/Cr(CN)_6^{-3}$. Ideally, the couples were to be tested on gold and graphite electrodes at 80° and 120°F, reduced to oxidized ratios of 1:10, 1:1 and 10:1 and total concentrations of 1M, 3M and 6M. In actual testing, solubility and corrosion effects frequently limited the range of conditions.

The results from Phase I showed the more promising couples to be: Fe^{+2}/Fe^{+3}, Br^{-}/Br_3^{-}, Ti^{+3}/Ti^{IV}, Cr^{+2}/Cr^{+3} and $Cu(NH_3)_2^{+1}/Cu(NH_3)_4^{+2}$. The Fe^{+2}/Fe^{+3} and Br^{-}/Br_3^{-}, couples were chosen as positive electrodes for their high exchange current densities and reasonable solubility limits; Br^{-}/Br_3^{-} also has a very high OCV for operation as a positive electrode. The Cr^{+2}/Cr^{+3} and $Cu(NH_3)_2^{+1}/Cu(NH_3)_4^{+2}$ couples were chosen for study, as negative electrodes, due to their reasonably high exchange current densities. (The titanium couple, although better than the chromium couple, was not chosen due to previous extensive study at NASA-Lewis.)

The second phase of the program involved the testing of these four couples in a redox reactor under flow conditions with a variety of electrode materials

and structures. The best performance with the negative electrode couples was obtained with the $Cu(NH_3)_2^{+1}/Cu(NH_3)_4^{+2}$ couple, particularly using a gold screen electrode in a frontal structure (i.e. electrode placed against the ion exchange membrane with electrolyte flowing on the back). The best performance with the positive electrode couples was obtained with the Br^-/Br_3^- couple, particularly with a porous carbon electrode in a recessed structure. The Fe^{+2}/Fe^{+3} couple using a graphite woven cloth electrode (as has been studied by NASA-Lewis) also showed very good performance.

I. TASK I - FIRST STAGE OF SCREENING OF REDOX COUPLES

A. INTRODUCTION

The first phase of this program involved a broad investigation of the physical and electrochemical characteristics of eight redox couples in order to compare their relative suitability for use in a redox fuel cell system. The eight couples chosen for study were the following: Fe^{+2}/Fe^{+3}, Sn^{+2}/Sn^{+4}, Sb^{+3}/Sb^{+5}, Ti^{+3}/Ti^{IV}, $Cu(NH_3)_2^{+1}/Cu(NH_3)_4^{+2}$, Cr^{+2}/Cr^{+3}, $Cr(CN)_6^{-4}/Cr(CN)_6^{-3}$, and Br^-/Br_3^-. The physical parameters that were measured were the degree of solubility in the recommended supporting electrolyte, the viscosity, and the conductivity. The solubility goals were 1M, 3Mand 6M total ion concentration at the reduced-to-oxidized ratios of 1:10, 1:1 and 10:1. The exchange current densities for the couples on both gold and vitreous carbon electrodes at 27°C and 50°C were determined using the rotating disk technique.

B. SOLUBILITY, VISCOSITY AND CONDUCTIVITY DETERMINATIONS

1. Experimental Procedures

a. Solubility

The preparation of solutions turned out to be a very difficult and time-consuming task. It appears that the reduced forms of these redox couples tend to be less soluble than the oxidized forms and more prone to hydrolysis. It was also necessary to maintain an inert atmosphere over most of the solutions at all times, which added to the complexity of the procedure. An additional variable was the supporting electrolyte concentration. For example, the acid levels anticipated in the Statement of Work did not turn out to be universally applicable over

the whole range of concentrations and redox ratios for the couples investigated. Therefore, it was necessary to test various acid concentrations to see which one was applicable to the widest rango of redox couple concentrations.

b. Viscosity

Viscosity measurements were made with Cannon-Fenske type viscometers, with openings modified as shown in Figure 1 to accommodate solution transfer to and from the cell. Two units were used with the following ranges: 0.8-4 centistokes and 3-15 centistokes. The measurements were made by drawing the appropriate quantity of solution into the viscometer (under N_2) and then placing it in the circulation chamber of the Haake Temperature Controller. After $\sim$ 10 minutes of equilibration, the time of flow between the two calibrated marks on the unit was measured.

c. Conductivity

Conductivities of the redox couple solutions were measured by a four point method using the apparatus shown in Figure 2. This apparatus was inserted through the cell cover, and the solution was drawn up to the bulb (over the Pt disk at the top). A small constant current was then passed between the upper electrod and the cell counter electrode at the bottom of the jacketed vessel (see Figure 3). A voltage recording device (either the strip chart recorder or oscilloscope) was connected to the two small Pt probes, and the voltage change was measured between zero current flow and the constant current flow. The solution resistance thus obtained was converted to specific conductance using a cell constant determined with 1N HCl.

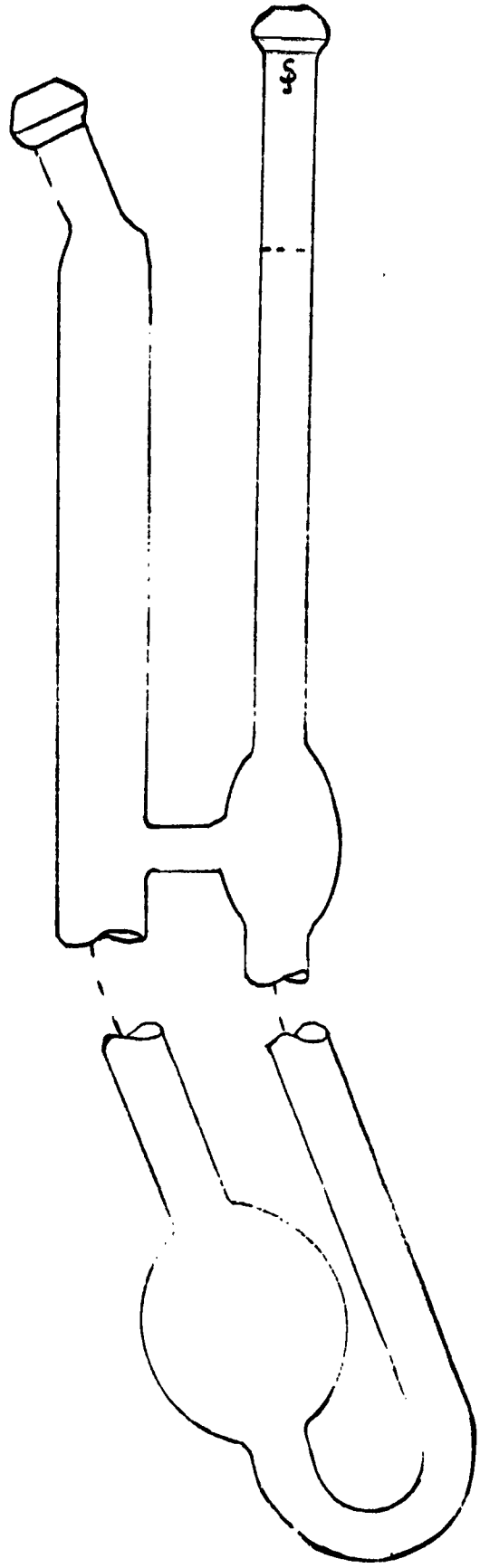

Figure 1. Viscometer

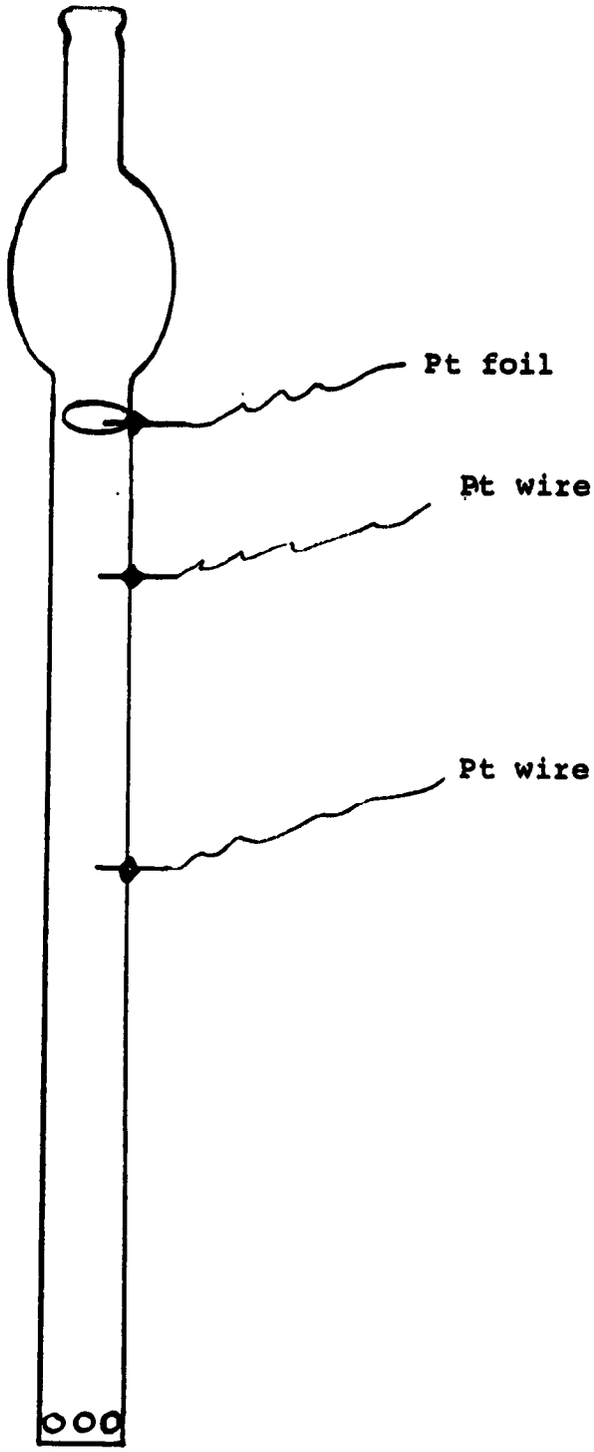

Figure 2. Apparatus for Conductivity Measurements.

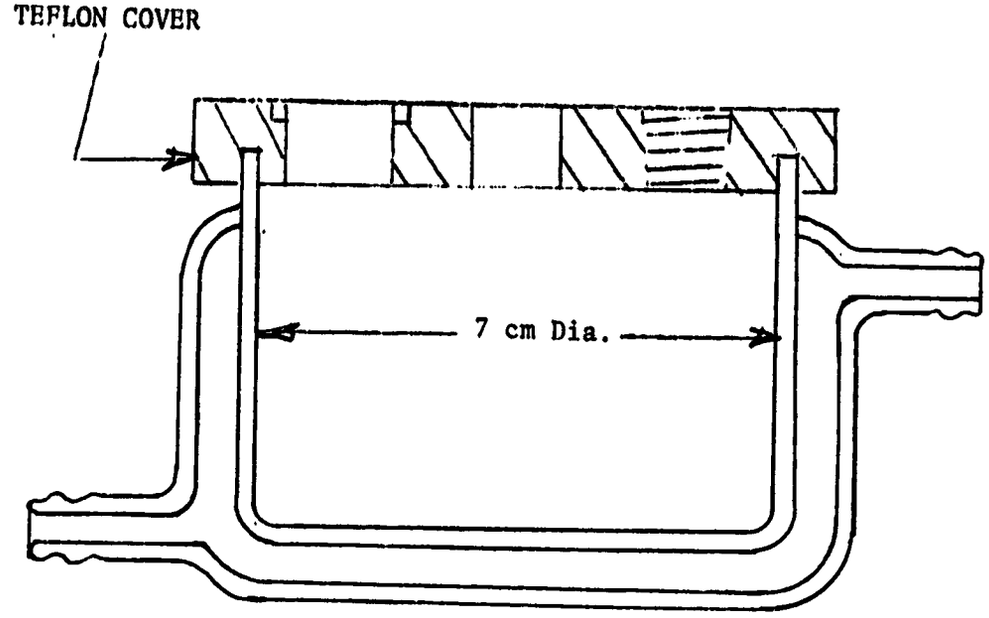

JACKETED VESSEL

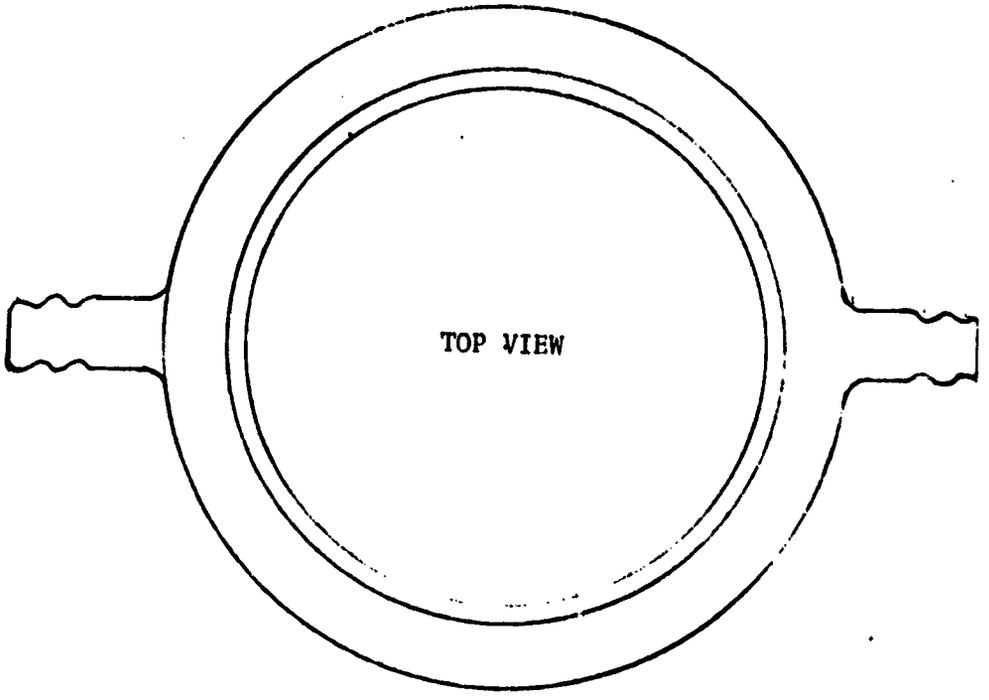

FIGURE 3. Electrochemical Cell.

2. Results

a. Fe^{+2}/Fe^{+3} (1N HCl)

Summary of Solubility

Red/Ox	1M	3M	4M	6M
1/10	sol.	sol.	sol.	--
1/1	sol.	sol.	insol.	insol.
10/1	sol.	sol.	insol.	--

For Fe^{+2}/Fe^{+3}, 1N HCl was used as the acid concentration for solution preparation. With this couple it was found that 6M Fe^{+2}/Fe^{+3} in any ratio could not be dissolved. The highest concentration suitable for all redox ratios was 3M, with 4M soluble only in the 1:10 redox ratio.* 4M 1:1 composition was attempted twice and after prolonged heating and stirring a 4M solution was obtained. However, analysis of both of the solutions showed a ratio of 1.4M Fe^{+2}/2.6M Fe^{+3}, indicating that the apparent solubility was a result of the Fe^{+2} being oxidized to the Fe^{+3} during the extended dissolution process (several days). The solutions prepared successfully along with their viscosities and conductivities, measured at 27°C and 50°C, are shown in Table I and graphed in Figure 4.

b. Sn^{+2}/Sn^{+4} (3.5N HCl)

Summary of Solubility

Red/Ox	1M	3M	5M	6M
1/10	sol.	sol.	sol.	insol.
1/1	sol.	sol.	sol.	insol.
10/1	sol.	sol.	sol.	insol.

Attempts to dissolve the Sn^{+2}/Sn^{+4} couple in 1N HCl were unsuccessful.

*All the redox ratios in this report are the ratio of the reduced to the oxidized species.

TABLE I. SPECIFIC CONDUCTANCE & VISCOSITY FOR FERROUS/FERRIC SOLUTIONS AT 27°C AND 50°C

Temperature °C	Parameter Measured (ohm-cm^{-1}) (centistokes)	Reduced/Oxidized Ratio at 1M Fe^{+2}/Fe^{+3} (in 1N HCl)		
		0.091M Fe^{+2} / 0.909M Fe^{+3}	0.5M Fe^{+2} / 0.5M Fe^{+3}	0.909M Fe^{+2} / 0.091M Fe^{+3}
27°	sp.cond.	0.262	0.291	0.314
	viscosity	1.50	1.34	1.20
50°	sp.cond.	0.347	0.393	0.407
	viscosity	1.02	0.94	0.84

		Reduced/Oxidized Ratio at 3M Fe^{+2}/Fe^{+3} (in 1N HCl)		
		0.27M Fe^{+2} / 2.72M Fe^{+3}	1.5M Fe^{+2} / 1.5M Fe^{+3}	2.72M Fe^{+2} / 0.27M Fe^{+3}
27°	sp.cond.	0.101	0.138	0.176
	viscosity	4.21	2.95	2.51
50°	sp.cond.	0.154	0.198	0.256
	viscosity	2.25	1.90	1.57

		Reduced/Oxidized Ratio at 4M Fe^{+2}/Fe^{+3} (in 1N HCl)		
		0.33M Fe^{+2} / 3.6M Fe^{+3}	1.4M Fe^{+2} / 2.6M Fe^{+3}	3.6M Fe^{+2} / 0.36M Fe^{+3}
27°	sp.cond.	0.070	0.090(1)	--(2)
	viscosity	5.20	4.78	--
50°	sp.cond.	0.120	0.135	--
	viscosity	2.71	2.78	--

1) This composition was soluble, but analysis indicates incorrect ratio. A second attempt at this preparation gave similar results.

2) Composition insoluble at this level of ferrous ion.

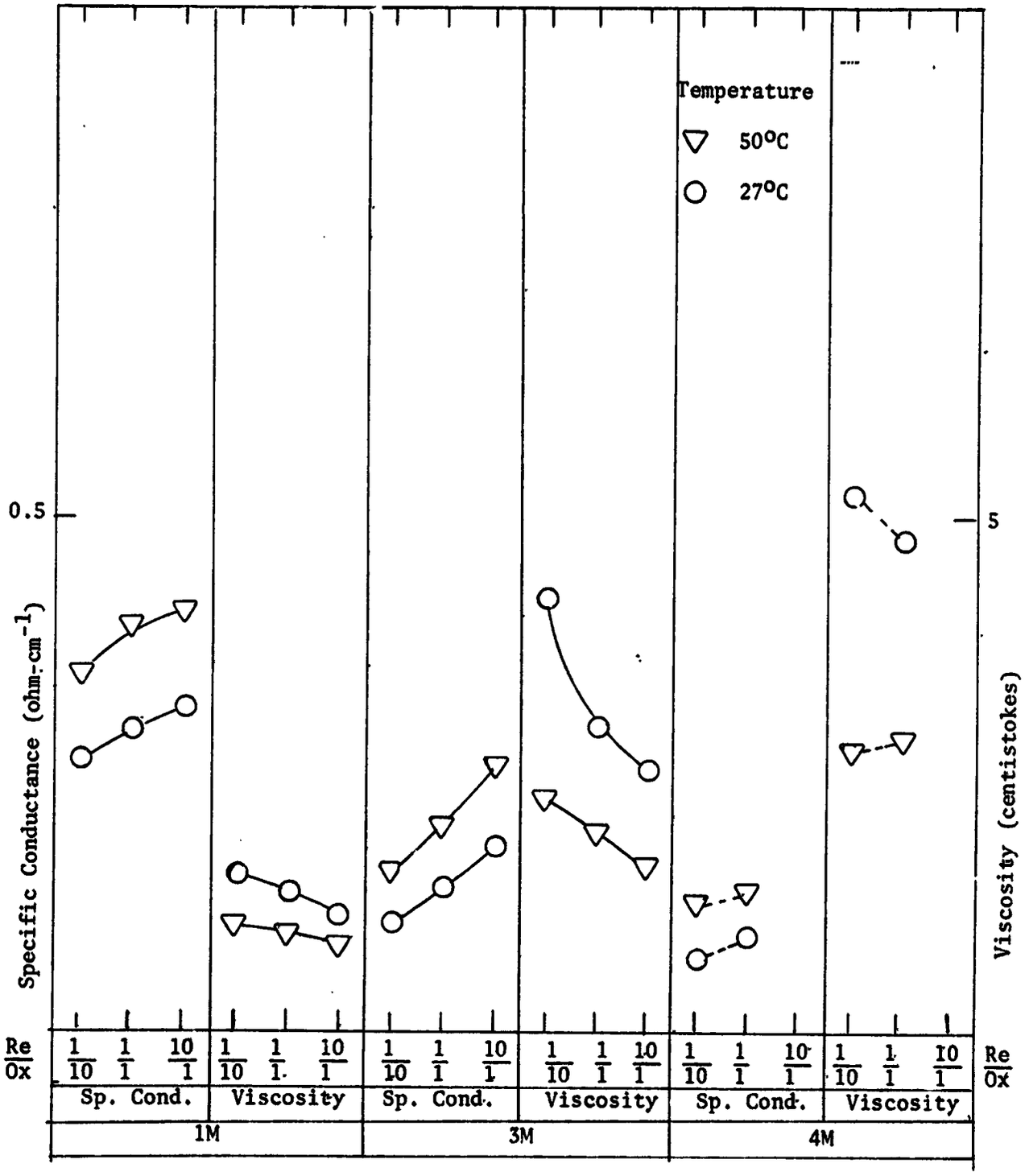

FIGURE 4. Specific Conductance and Viscosity for Fe^{+2}/Fe^{+3} (1N HCl).

Even low Sn concentration solutions became very cloudy and colloidal upon standing. Therefore, higher acid concentrations were investigated. 2N HCl also was not suitable, but with 3.5N HCl we were able to dissolve over 5M Sn^{+2}/Sn^{+4}. Therefore, we chose to stay at 3.5N HCl and use 5M Sn^{+2}/Sn^{+4} as the upper limit of solution concentration. The solutions that were prepared were 1, 3 and 5M Sn^{+2}/Sn^{+4} at 1:10, 1:1 and 10:1 redox ratios. Soluble compositions and values measured for viscosity and conductivity at 27°C and 50°C are shown in Table II and Figure 5.

c. Sb^{+3}/Sb^{+5} (3N HCl)

Summary of Solubility

Red/Ox	1M	3M	6M
1/10	sol.	sol.	insol.
1/1	sol.	sol.	sol.
10/1	insol.	insol.	insol.

3N HCl was specified in the Work Plan as the supporting electrolyte for the Sb^{+3}/Sb^{+5} couple, so initial attempts with solution preparation were done with this concentration. The 6M Sb^{+3}/Sb^{+5} (1:1) solution was soluble, so it was assumed that all other compositions could be prepared. However, it was found that, upon standing, the 10:1 redox couple composition precipitated. Lack of time prevented investigating a higher acid concentration. Therefore, the five soluble compositions were prepared and tested. The five solutions prepared along with the viscosity and conductivity for each solution at 27°C and 50°C are shown in Table III and Figure 6.

TABLE II. SPECIFIC CONDUCTANCE & VISCOSITY FOR STANNOUS/STANNIC SOLUTIONS AT 27°C AND 50°C

Temperature °C	Parameter Measured (ohm-cm^{-1}) (centistokes)	Reduced/Oxidized Ratio at 1M Sn^{+2}/Sn^{+4} (in 3.5 N HCl)		
		0.091M Sn^{+2} / 0.909M Sn^{+4}	0.5M Sn^{+2} / 0.5M Sn^{+4}	0.909M Sn^{+2} / 0.091M Sn^{+4}
27°	sp. cond.	0.590	0.717	0.852
	viscos.	1.26	1.10	1.06
50°	sp. cond.	0.786	0.830	0.985
	viscos.	0.83	0.78	0.72
		Reduced/Oxidized Ratio at 3M Sn^{+2}/Sn^{+4} (in 3.5 N HCl)		
		0.27M Sn^{+2} / 2.7M Sn^{+4}	1.5M Sn^{+2} / 1.5M Sn^{+4}	2.7M Sn^{+2} / 0.27M Sn^{+4}
27°	sp. cond.	0.265	0.389	0.616
	viscos.	2.52	1.69	1.24
50°	sp. cond.	0.378	0.515	0.715
	viscos.	1.42	1.04	0.87
		Reduced/Oxidized Ratio at 5M Sn^{+2}/Sn^{+4} (in 3.5 N HCl)		
		0.454M Sn^{+2} / 4.54M Sn^{+4}	2.5M Sn^{+2} / 2.5M Sn^{+4}	4.54M Sn^{+2} / 0.454M Sn^{+4}
27°	sp. cond.	0.063	0.176	0.378
	viscos.	9.81	3.95	1.85
50°	sp. cond.	0.105	0.249	0.481
	viscos.	4.43	2.19	1.23

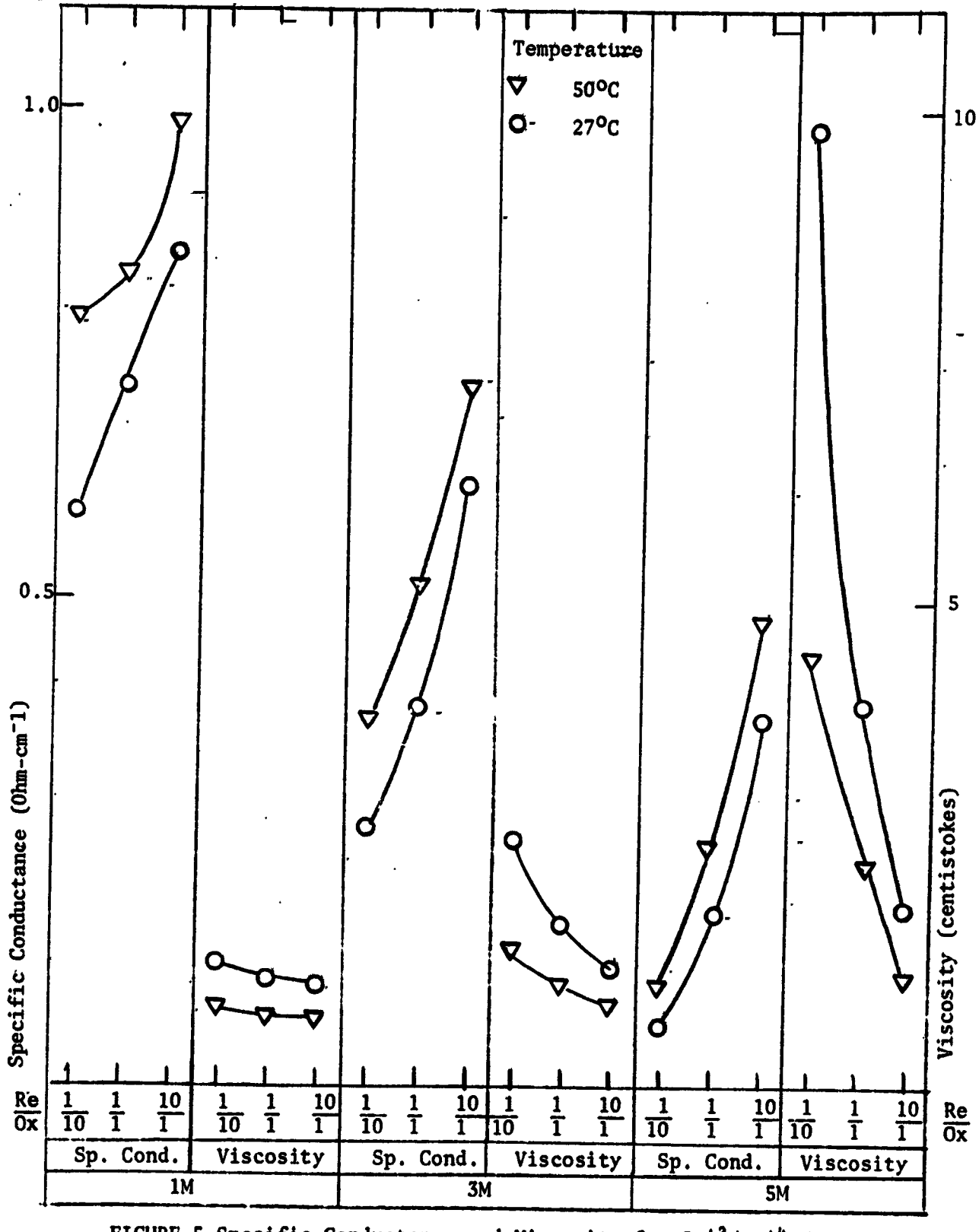

FIGURE 5-Specific Conductance and Viscosity for Sn^{+2}/Sn^{+4} (3.5N HCl)

TABLE III. SPECIFIC CONDUCTANCE AND VISCOSITY FOR ANTIMONY^{+3}/ANTIMONY^{+5} SOLUTION AT 27°C AND 50°C

Temperature °C	Parameter Measured ($ohm\text{-}cm^{-1}$) (centistokes)	Reduced/Oxidized Ratio at 1M Sb^{+3}/Sb^{+5} (in 3N HCl)		
		0.091M Sb^{+3} / 0.909M Sb^{+5}	0.5M Sb^{+3} / 0.5M Sb^{+5}	0.909M Sb^{+3} / 0.091M Sb^{+5}
27°	sp. cond.	0.674	0.750	0.779 (1)
	viscosity	1.35	1.28	1.14
50°	sp. cond.	0.889	0.937	0.980 (1)
	viscosity	1.013	1.09	0.79

		Reduced/Oxidized Ratio at 3M Sb^{+3}/Sb^{+5} (in 3N HCl)		
		0.27M Sb^{+3} / 2.7M Sb^{+5}	1.5M Sb^{+3} / 1.5M Sb^{+5}	2.7M Sb^{+3} / 0.27M Sb^{+5}
27°	sp. cond.	0.334	0.440	--(2)
	viscesity	2.45	2.30	--
50°	sp. cond.	0.473	0.598	--
	viscosity	1.48	1.31	--

		Reduced/Oxidized Ratio at 6M Sb^{+3}/Sb^{+5} (in 3N HCl)		
		0.545M Sb^{+3} / 5.45M Sb^{+5}	3.0M Sb^{+3} / 3.0M Sb^{+5}	5.45M Sb^{+3} / 0.545M Sb^{+5}
27°	sp. cond.	--(3)	0.092	--(4)
	viscosity	----	4.53	--
50°	sp. cond.	--	0.138	--
	viscosity	--	2.35	--

1) This composition was soluble initially but precipitated after standing a few days. A repeat preparation yielded the same results.
2) This composition precipitated.
3) Not soluble.
4) Not prepared.

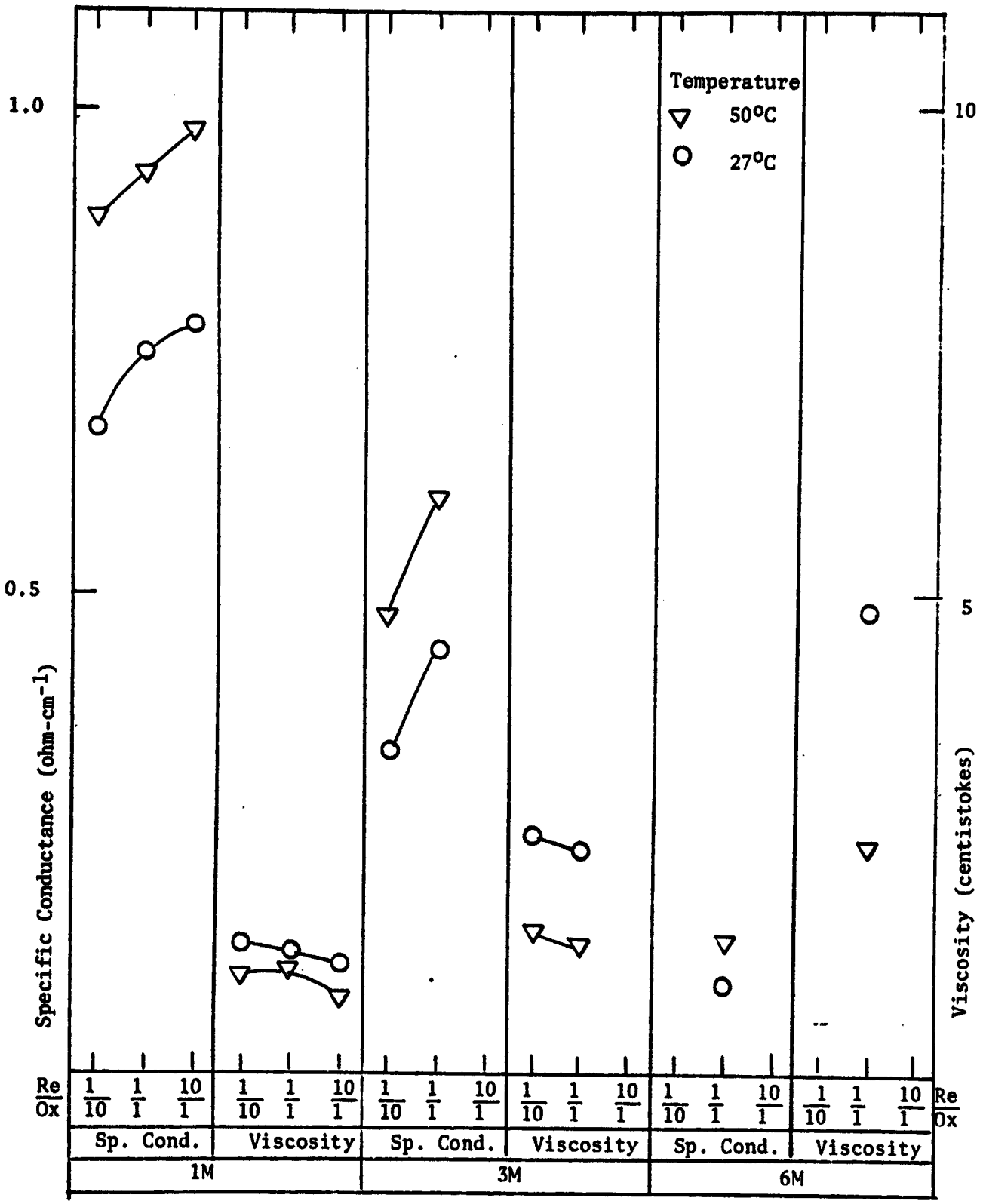

FIGURE 6. Specific Conductance and Viscosity for Sb^{+3}/Sb^{+5} (3N HCl).

d. Ti^{+3}/Ti^{+4} (6M HCl)

Summary of Solubility

Red/Ox	1M	3M	6M
1/10	sol.	sol.	insol.
1/1	sol.	sol.	insol.
10/1	sol.	sol.	insol.

Ti^{+3}/Ti^{+4} solutions of 1M and 3M Ti concentrations with redox ratios of 1:10, 1:1 and 10:1 were prepared in 6N HCl, the acid concentration specified in the Work Plan. The 6M composition was found to be insoluble (< 4M max.). The solution concentrations prepared along with measured viscosities and conductivities at 27°C and 50°C are shown in Table IV and Figure 7.

e. $Cu(NH_3)_2^{+1}/Cu(NH_3)_4^{+2}$ (1M NaCl + 0.01M NaOH)

Summary of Solubility

Red/Ox	1M	3M
1/10	sol.	sol.
1/1	sol.	sol.
5/1	sol.	insol.
10/1	insol.	insol.

In the preparation of solutions of the $Cu(NH_3)_2^{+1}/Cu(NH_3)_4^{+2}$ couple, the reduced form of the couple was found to have low solubility. Seidell[1] indicates a very low solubility for cuprous chloride alone in water, 0.01-0.1%. In the presence of cupric chloride the solubility increases as shown below:

Solubility of $CuCl/CuCl_2$ in H_2O at 19°C (sat'd)

CuCl (m/l)	$CuCl_2$ (m/l)	Red/Ox
.16	1.0	1/6.25
.41	1.93	1/4.8
.64	3.23	1/5
.80	4.0	1/5
.88	4.9	1/5.5

TABLE IV. SPECIFIC CONDUCTANCE & VISCOSITY FOR Ti^{+3}/Ti^{IV} SOLUTIONS AT 27°C AND 50°C

Temperature °C	Parameter Measured ($ohm\text{-}cm^{-1}$) (centistokes)	Reduced/Oxidized Ratio at 1M Ti^{+3}/Ti^{IV} (in 6N HCl)		
		0.091M / 0.909M	0.5M / 0.5M	0.909M / 0.091M
27°	sp. cond.	0.658	0.598	0.562
	viscosity	1.67	1.913	1.83
50°	sp. cond.	0.860	0.727	0.708
	viscosity	1.21	1.26	1.24

		Reduced/Oxidized Ratio at 3M Ti^{+3}/Ti^{IV} (in 6N HCl)		
		0.27M / 2.7M	1.5M / 1.5M	2.7M / 0.27M
27°	sp. cond.	0.301	0.272	0.207
	viscosity	4.99	5.15	5.28
50°	sp. cond.	0.395	0.356	0.252
	viscosity	3.13	3.13	3.29

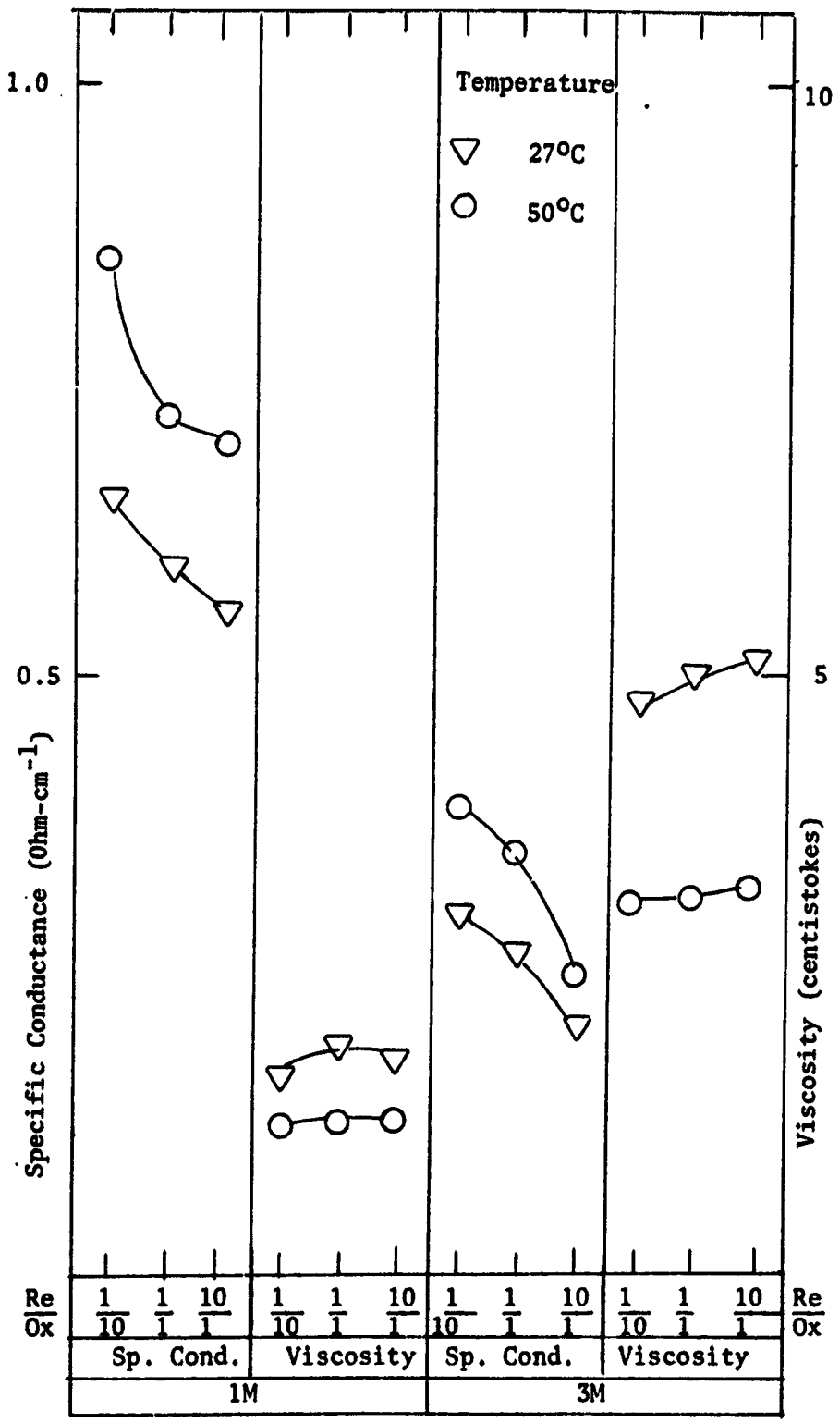

FIGURE 7. Specific Conductance and Viscosity for Ti^{+3}/Ti^{IV} (6N HCl) Solutions.

Complexing with ammonia improves the solubility to 1:1 at 3M total concentration. This level of solubility of the cuprous ion, 1.5 mol/ℓ, would seem to favor the possibility of a 10:1 ratio at a total concentration of 1 mol/ℓ, but some dependence on cupric ion concentration apparently is retained even for the complexed ions.

In our preparation, NH_4OH (27% NH_3) was used as the solvent. Also the method of bubbling pure NH_3 gas over the Cu^{+1}/Cu^{+2} was employed to help dissolution. However, concentrations higher than 3M Cu could not be obtained and the 10:1 (Red/Ox) in the 1M or 3M Cu could not be prepared.

A second preparation of the 10:1 (Red/Ox) 1M and 3M compositions was attempted in order to investigate the solubility further. After make-up with $CuCl/CuCl_2$ and NH_4OH, the solutions were heated and stirred continuously with NH_3 gas bubbling through the solution for 30 minutes. The compositions remained insoluble, however. A 5:1 composition at 1M total concentration was soluble, and this was chosen as the upper limit for further investigation. It is to be noted that the reduced form of the complex has less NH_3 than the oxidized, so that the solubility problem of the 10:1 solutions is not due to a lack of NH_3. We were able to prepare 1 and 3M $Cu(NH_3)_2^{+1}/Cu(NH_3)_4^{+2}$ in the redox ratios of 1:10 and 1:1 and 1M 5:1. The solutions prepared with their measured viscosities and conductivities at 27°C and 50°C are shown in Table V and Figure 8.

f. Cr^{+2}/Cr^{+3} (1M HCl)

Summary of Solubility

Red/Ox	∿ 1M
0.08/0.91	sol.
0.33/0.5	sol.

TABLE V. SPECIFIC CONDUCTANCE AND VISCOSITY FOR

$Cu(NH_3)_2^{+1}/Cu(NH_3)_4^{+2}$ SOLUTIONS AT 27°C AND 50°C

Temperature °C	Parameter Measured (ohm-cm^{-1}) (centistokes)	Red/Ox Ratio at 1M Conc. (Sat'd. NH_4OH) 0.091M / 0.909M	0.5M / 0.5M	0.833M / 0.167M
27°	sp. cond.	0.124	0.096	0.535
	viscosity	1.23	1.12	1.51
50°	sp. cond.	0.226	0.131	0.867
	viscosity	0.89	0.78	0.97

		Red/Ox Ratio at 3M Conc. (Sat'd. NH_4OH) 0.27M / 2.7M	1.5M / 1.5M
27°	sp. cond.	0.231	0.202
	viscosity	1.44	1.66
50°	sp. cond.	0.271	0.228
	viscosity	1.09	1.15

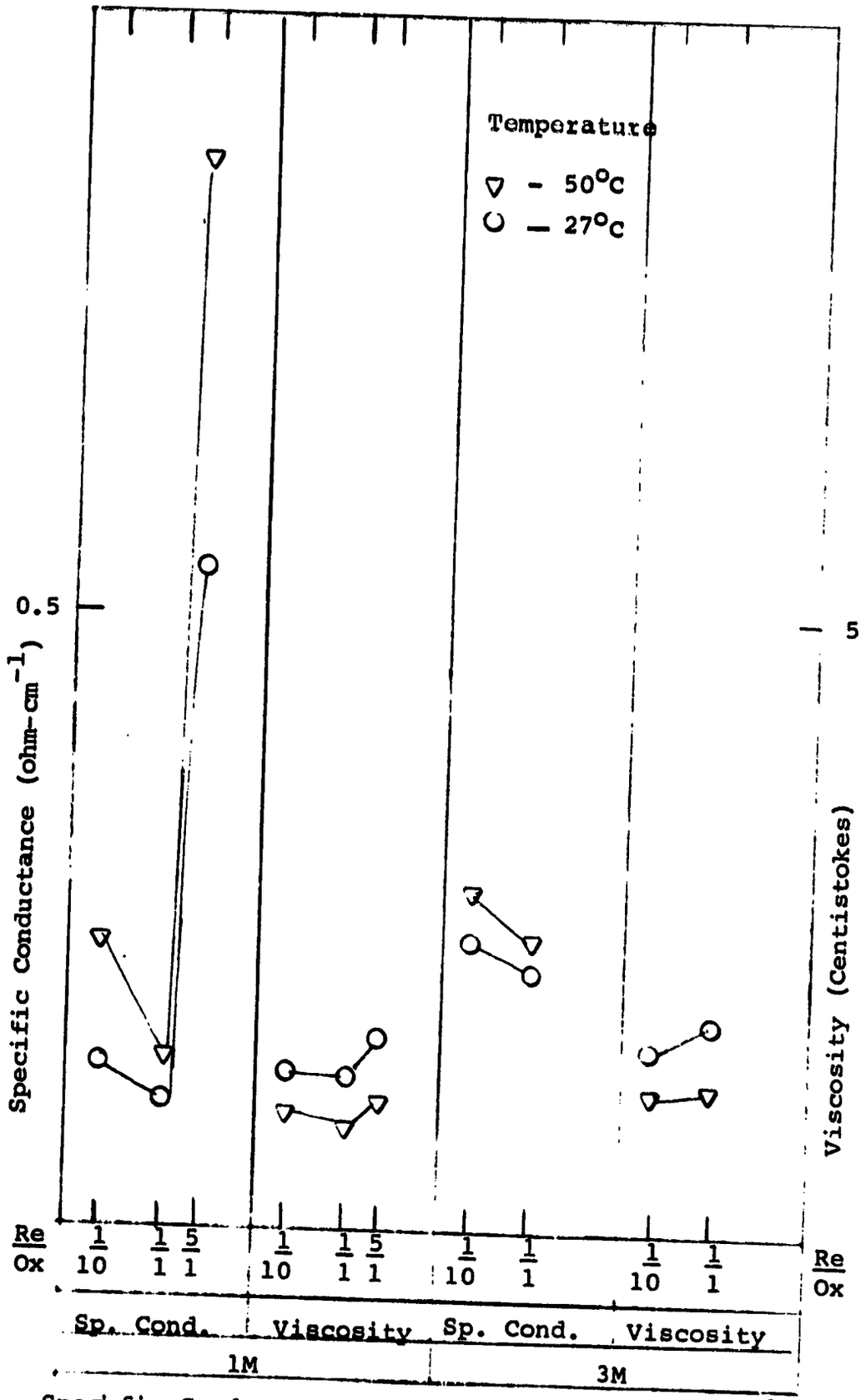

Figure 8. Specific Conductance and Viscosity for $Cu(NH_3)_2^{+1}/Cu(NH_3)_4^{+2}$ Solutions.

Attempts to dissolve $CrCl_2$ in HCl showed considerable difficulty. Various brands of the compound were purchased, but very low solubility was obtained in all cases. A small sample of $CrCl_2$ (Fisher Scientific) was obtained from NASA-Lewis for comparison with the materials we had been using. It was observed to be light gray in color in contrast to a light green color for our materials and was found to be more soluble than the material we obtained from Fisher or Ventron. Using the Fisher material obtained from NASA-Lewis, we were able to prepare two ∿ 1M Cr solutions; 0.081M (out of 0.09M Cr^{+2} added) and 0.33M Cr^{+2} (out of 0.5M Cr^{+2} added). It seemed probable that part of the problem was the impurity level of the chromous chloride salt, the impurities being something other than $CrCl_3$, since there was an insoluble residue even after vigorous heating and stirring.

The viscosities and conductivities at 27°C and 50°C for the two solutions prepared are shown in Table VI and Figure 9.

g. Br^-/Br_3^- (NaBr)

With regard to the Br^-/Br_3^- couple, the solubility data available in the literature was examined to determine the feasible operating concentration range. The maximum solubility of NaBr in H_2O at 25°C is ∿ 7.3M.[2] The solubility of bromine (Br_2-partial pressure not stated) in aqueous sodium bromide at 25°C (which limits the maximum charged state of the couple) is as follows:

NaBr (aq.)	Br_2 (aq.)
0.9 moles/ℓ	0.62 moles/ℓ
1.56	1.10
2.00	1.55
3.10	3.41
3.48	4.01
4.0	5.2

TABLE VI. SPECIFIC CONDUCTANCE AND VISCOSITY FOR Cr^{+2}/Cr^{+3} SOLUTIONS AT 27°C AND 50°C

Temperature	Parameter	Red/Ox Ratio at ~ 1M (1M HCl)	
°C	(ohm-cm^{-1}) (centistokes)	0.081M / 0.909M	0.33M / 0.50M
27°	Sp. Cond.	0.226	0.178
	Viscosity	1.83	1.56
50°	Sp. Cond.	0.310	0.239
	Viscosity	1.21	1.09

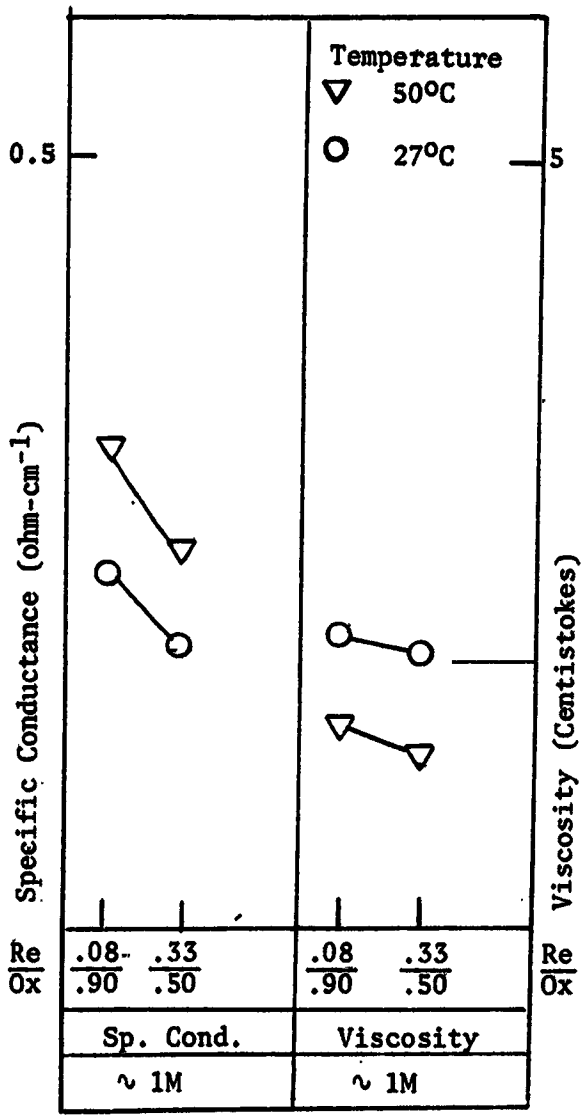

FIGURE 9: Specific Conductance and Viscosity for Cr^{+2}/Cr^{+3} Solutions.

The following solutions were prepared for our measurements:

Summary of Solubility

High Level (Total Br = 9 g-atom ℓ^{-1})	Low Level (Total Br = 2.1 g-atom ℓ^{-1})
Br^-/Br_3^-	Br^-/Br_3^-
6.3M/0.9M	1.5M/0.2M
3M/2M	0.9M/0.4M
0M/3M	0.3M/0.6M

The viscosities and conductivities values are shown in Table VII and Figure 10.

h. $Cr(CN)_6^{-4}/Cr(CN)_6^{-3}$ (NaCl)

We attempted to prepare a 1M 1:1 composition of this couple by dissolving chromous chloride in 6M NaCN. The chromous complex appeared to be almost completely insoluble. Very little solubility data is available for this couple. The Handbook of Chemistry[3] indicates a moderate solubility for the chromic complex, $\sim$ 0.1 moles $K_3 Cr(CN)_6/100g\ H_2O$.

Randles and Somerton[4] investigated this couple but only with concentrations of 10^{-3}M, and they give no indication of their method of preparation. Hume and Kolthoff[5] also investigated this couple again at about 10^{-3}M. They first attempted to prepare the chromous complex by adding potassium cyanide to electrolytically prepared chromous chloride. They do not indicate the amount of chromocyanide obtained, if any, but report the formation of a small amount of reddish brown precipitate. Their preferred method was the electrolytic reduction of 0.01 or 0.1M chromicyanide on mercury. They were able to obtain up to 75% reduction by this method ($\sim$ 0.075M chromocyanide) before changing completely to hydrogen evolution. They report that the chromous complex is highly unstable (less stable than the chromicyanide ion by a factor of 10^{12}).

TABLE VII. SPECIFIC CONDUCTANCE AND VISCOSITY FOR Br^-/Br_3^- SOLUTIONS AT 27°C

Temperature	Parameter Measured	Total Br, g-atom/ℓ^{-1} (Red/Ox Ratio)		
		2.1(0.3M/0.6M)	2.1(0.9M/0.4M	2.1(1.5M/0.2M)
27°C	Sp. Cond. (ohm-cm^{-1})	0.092	0.120	0.145
	Viscosity (centistokes)	0.89	0.89	0.93
		9(0M/3M)	9(3M/2M)	9(6.3M/0.9M)
27°C	Sp. Cond. (ohm-cm^{-1})	0.216	0.260	0.269
	Viscosity (centistokes)	0.98	1.22	1.52

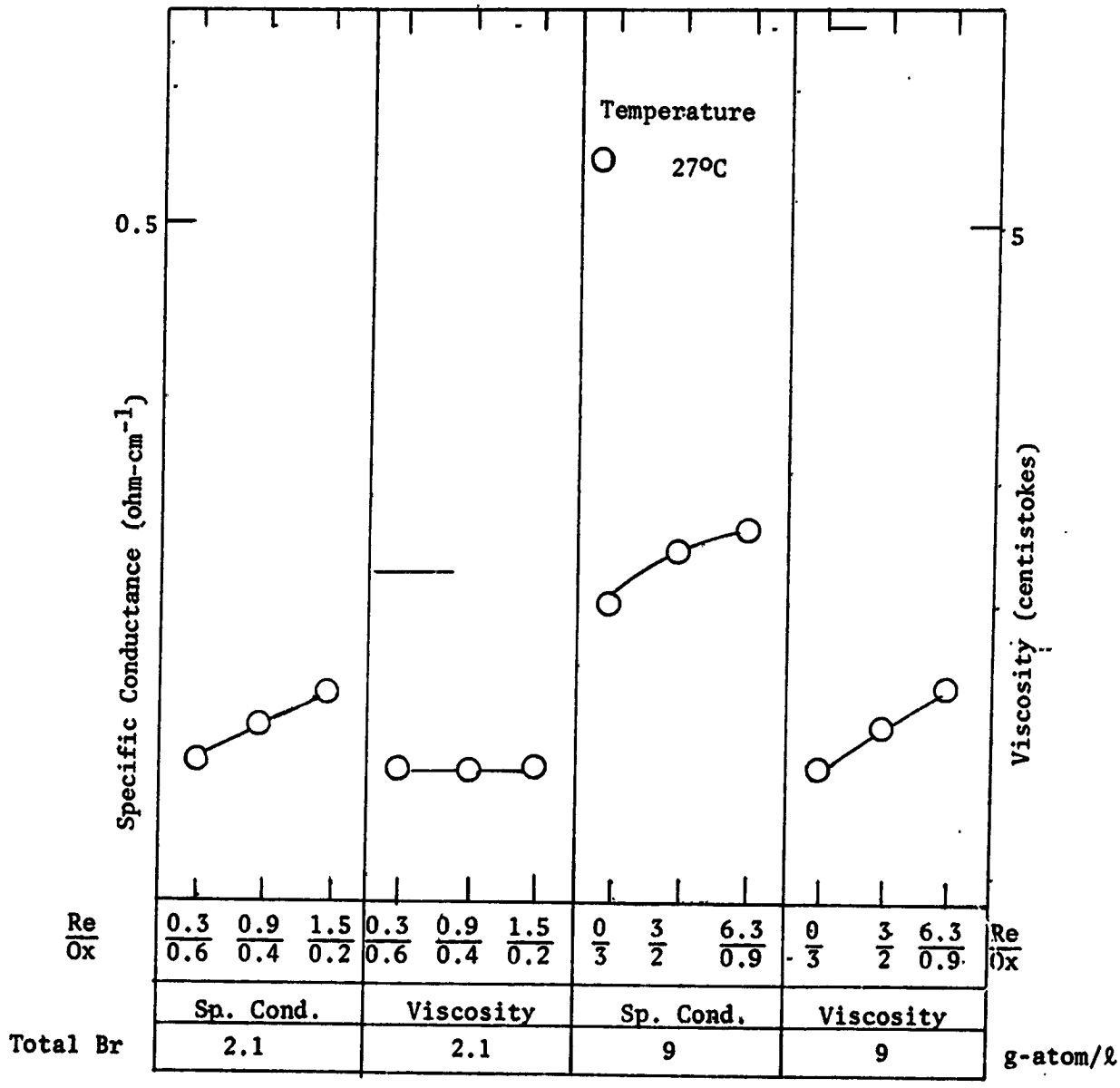

FIGURE 10. Specific Conductance and Viscosity for Br^-/Br_3^- Solutions.

Based on this low solubility for the couple and the instability of the chromocyanide ion, we concluded that this couple probably was not suitable for redox cell application in spite of the relatively high exchange current density reported ($\sim$ 24 mA/cm^2 at 10^{-3}M on Hg) and a very negative potential ($\sim$ - 1.0V).[6]

C. EXCHANGE CURRENT DENSITY MEASUREMENTS

1. Theoretical Background

The exchange current of a redox couple can be obtained under ideal conditions by extrapolating the linear portion of log i vs. polarization plots (Tafel plots) and determining the current at which the so extrapolated anodic and cathodic plots intercept, if both Tafel plots are used; or by determining the extrapolated current at the thermodynamic open circuit potential, if only one of these Tafel plots is used.

In practice the length of the linear portion of the Tafel plot is limited by the back reaction, by concentration polarization and by ohmic polarization. Ohmic polarization can be taken into account by using for instance, an interrupter technique; as a consequence, the polarization can be corrected for this contribution according to:

$$\eta_{corr} = \eta - iR \qquad (1)$$

After this correction, the linear portion of the Tafel plot is still limited to polarizations higher than about 100 mV, by the back reaction, and to currents which are a small fraction of the limiting current i_L, by concentration polarizations. (This upper boundary can be increased by increasing stirring.)

In the case of very high exchange currents, for practical degrees-of stirring, the region of linearity can disappear or be so narrow as to make impossible the extrapolation of exchange currents based on Tafel plots of steady-state current and polarization data. Under these conditions, corrections for the back reaction and/or concentration polarizations have to be undertaken in order to extend the linear region of a Tafel plot. Such corrections can be performed by correcting the measured current as done by Essin (see page 465, ref. 6). His approach, used in this work,

leads to a correction of current given by equation:

$$i_{corr} = \frac{i_{meas}}{\left(1 - \frac{i_{meas}}{i_{La(c)}}\right) - \left(1 - \frac{i_{meas}}{i_{Lc(a)}}\right) \exp - \frac{F}{RT} \eta_{corr}} \qquad (2)$$

where, i_{meas} = uncorrected measured current either anodic or cathodic

$i_{La(c)}$ = anodic limiting current when i_{meas} is anodic, and cathodic limiting current when i_{meas} is cathodic

$i_{Lc(a)}$ = cathodic limiting current when i_{meas} is cathodic, and anodic limiting current when i_{meas} is anodic

η_{corr} = iR-corrected polarization, in absolute value

The first term in the denominator corrects for the effect of concentration polarization while the second term takes into consideration the back reaction. Within this second term, which becomes very small as η_{corr} becomes larger than 100 mV, the parenthesis takes into consideration the fact that for reactions with very high exchange current, there can be a considerable build up of the concentration of the reaction product close to the electrode, even for polarizations smaller than 100 mV.

Use of equation (2) requires that:

1. There is direct proportionality between current and concentration. (Such case will be the most probable in redox reaction involving a simple electron transfer.)

2. The diffusion layer remains constant throughout the measurement of the complete i-η curve. This requires well defined forced convection, such as obtained with a rotating disk.

3. The limiting current can be determined accurately for the used rotation either by direct measurement or by extrapolation. This condition

suggests again the use of RDE.

4. Ohmic-disturbances to ideal rotating disk electrode theory[7] are kept low. For this condition the reference electrode is kept far removed from the RDE.

5. Current-potentials points are selected to minimize corrections, because of unavoidable uncertainties in the determination of limiting currents and ohmic polarization. This condition mandates use of high rotation rates compatible with accurate determination of the limiting current, and places a limit in the magnitude of the current which can be used for the log i-η plots.

Another method to correct the current with help of the rotating disk technique, for use in a Tafel plot, is based on equation:

$$\frac{1}{i_{corr}} = \frac{1}{i_{meas}} - \frac{i}{i_L} \quad \ldots \quad (3)$$

or

$$\frac{1}{i_{corr}} = \frac{1}{i_{meas}} - \frac{1}{k\sqrt{\omega}} \quad (4)$$

where in addition to the previously introduced symbols, ω is the angular rotation speed of the rotating disk, and k is a constant.

In this method the current is measured at a given polarization (η_{corr}) for different rotation speeds. The intercept with the ordinate in a $\frac{1}{i_{meas}}$ vs. $\frac{1}{\sqrt{\omega}}$ plot produces $\frac{1}{i_{corr}}$, which can be used for the log i_{corr} vs. η_{corr} - Tafel plot.

We decided against the use of this approach in this work because equation (3) does not consider the back reaction (note that eq.(3) becomes identical with equation (2) when the second term in the denominator of eq.(2)

is disregarded), and forces to carry experiments towards high polarizations, i.e. towards high $\frac{i}{i_L}$ ratios for reactions with high exchange currents. In addition, the method is quite cumbersome since it requires the measurement of a number of complete i-η curves at different electrode rotations.

Instead of using the linear part of a plot of logarithm of current vs. polarization for determination of exchange currents, it is possible also to use a linear plot and to determine the slope at open circuit related to the exchange current by:

$$i_o = \frac{RT}{F}\left(\frac{i}{\eta}\right)_{\eta=0} \qquad (5)$$

When applying this approach to an electrode reaction of very high exchange current, it is again necessary to use very small polarizations (microvolts) so that i and, therefore, concentration and ohmic polarization remain small.

This approach was used in this work in a number of cases (Sb^{+3}/Sb^{+5}, Cr^{+2}/Cr^{+3}). This was done after having obtained the complete i-η curve, and having ascertained that the exchange current was low enough to allow for graphic determination of the slope at open circuit.

For completeness sake, non-steady state methods based on the controlled transient build up of the diffusion layer have to be mentioned here. These methods can successfully be used to correct for concentration polarization, but were not used in this work because they do not lend themselves for routine application when a very large number of exchange currents have to be determined.

2. Experimental Procedure

Preliminary measurements were carried out with the Fe^{+2}/Fe^{+3} couple to determine the appropriate range of data to be taken in determining i_o for the eight redox couples. The method used was the

rotating disk electrode technique obtaining I-E relationships either by applying linear potential sweeps or graduated potential steps to the test electrode up to the limiting currents for various rotation rates.

The electrochemical cell used for these experiments consisted of a jacketed vessel of ∿ 100 ml volume (7 cm diameter to give an electrode to cell diameter ratio of 1:8), with a fitted Teflon cover to accommodate the electrodes (see Figure 3). The RDE was inserted in the central opening and secured with a Teflon fitting. The reference electrode for polarization measurements was a saturated calomel, and it was inserted in one of the peripheral openings sealed with an "O" ring. For iR measurements it was necessary to use a platinized Pt probe as reference due to excessive noise with the calomel reference. The counter electrode was a gold ring at the bottom of the cell. A thermometer and gas inlet and outlet tubes were secured with Teflon Swagelok fittings. The temperature of the cell was controlled to ± 0.5°C by circulating water through the jacketed vessel from a Haake Temperature Controller. Nitrogen, to sweep the solution and cell chamber of air, was presaturated with water vapor to reduce water evaporation from the cell during operation. The proper temperature for the presaturator was approximated since little vapor pressure data was available for the redox couple solutions under investigation. The RDE was a Beckman Model No. 188501 variable speed drive assembly with rotational speeds variable from 3-100 rps. The specifications are as follows:

Concentricity:	± 0.0026"
Wobble:	± 0.008"
Accuracy of Rotational Speed:	± 1% above 3 rps
Repeatability of Rotational Speed:	± 10%

The test electrodes were gold (Beckman #39087) and vitreous carbon (Beckman #39084). The electrodes were interfaced to the drive assembly with Beckman Electrode Assemblies (#188551) through the flexible drive cable. The electrodes were polished (with 0.5 micron alumina) and the following surface roughness values were obtained: gold = 69 $\mu f/cm^2$, vitreous carbon = 29 $\mu f/cm^2$. A substitute drive assembly was also used. This consisted of a G.K. Heller variable speed stirrer motor and controller, Model GT-21 (0-100 rps). The drive shaft of this motor was coupled to the Beckman RDE electrode assembly, and the rotation speed was monitored with an oscilloscope by converting the off-times of an LED/photocell sensing circuit as it was interrupted by an opaque marker arm attached to the drive shaft.

The IR was measured by the current interruption method using a current density of $\sim$ 50 mA/cm^2 and monitoring the potential change with an oscilloscope trace at 1-2 msec/div. The reference electrode was a Pt probe as mentioned above.

The exchange current densities were obtained from the intercepts of plots of log i_{corr}. Polarizations were corrected for iR drop, and measured currents were corrected for the back reaction at low currents and for concentration polarization at high currents according to equation (2). Values for i_{corr} were determined from both anodic and cathodic curves whenever possible. A computer program was set up which calculated the values for i_{corr} and η_{corr}. Therefore, in order to obtain the desired I-E relationship both diffusion limiting current values and low polarization measurements were taken. We measured the limiting current at 3 rotation speeds whenever possible, 5 rps, 10 rps and 50 rps. This allowed verification according to the relationship $i_L = k\sqrt{\omega}$ where ω is the

angular rotation speed, k is a constant and i_L is the limiting current. For situations where values could not be measured at 50 rps, a value was calculated from the above relationship, using the values obtained at 5 rps. Current density data was taken at 50 rps at the following levels (mA): 0.1, 0.15, 0.3, 0.5, 1.0, 1.5, 3.0, 5.0, 10, etc. to 0.5 i_L.

3. Results

a. Fe^{+2}/Fe^{+3} (1N HCl)

The exchange current densities were determined for the seven soluble Fe^{+2}/Fe^{+3} solutions on both gold and carbon at 27°C and 50°C. A reliable exchange current density for gold in the 4M 1:10 ratio solution could not be derived from the experimental data, although the range of values indicated are of a consistent order of magnitude. The exchange current densities were obtained from the intercepts of plots of log i_{corr} versus η_{corr} according to Equation (2).

The values of i_o were determined from both the anodic and cathodic curves for each solution whenever possible. Both curves were generally in good agreement except for the 1:10 and 10:1 ratios at 1M total concentration. For these solutions the i_o value was based primarily on the cathodic curve for the 1:10 ratios and the anodic curve for the 10:1 ratios. The species at the lower concentration level in these cases is apparently too low (0.09M) for reliable measurement of the exchange current. The exchange currents and open circuit voltages for gold and carbon at 27°C and 50°C for the Fe^{+2}/Fe^{+3} are shown in Table VIII.

b. Sn^{+2}/Sn^{+4} (3.5N HCl)

I(E) measurements were determined for six of the nine compositions of the tin couple prepared (1 and 3M). This couple appears to be

TABLE VIII. EXCHANGE CURRENT DENSITY, -log i_o (A/cm^2)

Fe^{+2}/Fe^{+3} (1N HCl)

Total Concentration	Red/Oxid.	27°C Gold	27°C Carbon	50°C Gold	50°C Carbon
1M	1/10	1.6	2.5	1.3	2.2
	1/1	1.2	2.0	1.0	1.3
	10/1	1.5	2.2	1.3	1.7
3M	1/10	1.6	1.9	1.3	1.7
	1/1	1.0	1.5	0.8	1.3
	10/1	1.4	1.7	1.2	1.5
4M	1/10	~1.6	1.9	1.2	1.3
	1/1(insol)				
	10/1(insol)				

OPEN CIRCUIT VALUES - Fe^{+2}/Fe^{+3} (mV vs. SCE)

Total Concentration	Red/Oxid.	27°C Gold	27°C Carbon	50°C Gold	50°C Carbon
1M	1/10	507	508	530	530
	1/1	448	447	467	462
	10/1	386	386	399	397
3M	1/10	490	490	510	510
	1/1	433	432	444	444
	10/1	371	367	378	378
4M	1/10	501	482	512	512

fairly irreversible. Very little current is observed corresponding to the reaction $Sn^{+4} + 2e^{+} \rightarrow Sn^{+2}$ ($\sim$ 0.14V vs. SHE). This was at most $\sim$ 8 mA/cm^2 seen as a small peak, rather than a limiting current with gold; no measurable cathodic current was observed with carbon. Beyond this small current peak a large increase in current was observed corresponding visually with tin plating on gold; on carbon a fine precipitate formed at the electrode surface.

The anodic reaction occurred with much less polarization. Polarization data and anodic limiting currents were obtained with carbon in most cases, from which exchange currents were derived. On gold, however, no unambiguous limiting currents were obtained. During the anodic sweep on gold a sharp drop in current was regularly observed, possibly indicating passivation of the surface of the electrode, followed by a second slow rise in current to a higher plateau. Typical curves obtained for Sn^{+2}/Sn^{+4} on gold and carbon are shown in Figure 11.

Our results are in agreement with those of Lerner and Austin,[8] who investigated the tin couple (on carbon), and report that it reacts fairly irreversibly according to a two-step process:

$$Sn^{+2} \rightarrow Sn^{+3} + e^{-} \qquad \text{(a)}$$

$$\underline{Sn^{+3} \rightarrow Sn^{+4} + e^{-}} \qquad \text{(b)}$$

$$Sn^{+2} \rightarrow Sn^{+4} + 2e^{-}$$

They indicate that step (b) is rate controlling at η = 30 to 120 mV, and step (a) is rate controlling from η = 240 mV to 0.1 i_L. Because of the apparent irreversibility of the Sn^{+2}/Sn^{+4} reaction, our calculations of exchange currents were limited to anodic data. The anodic data were

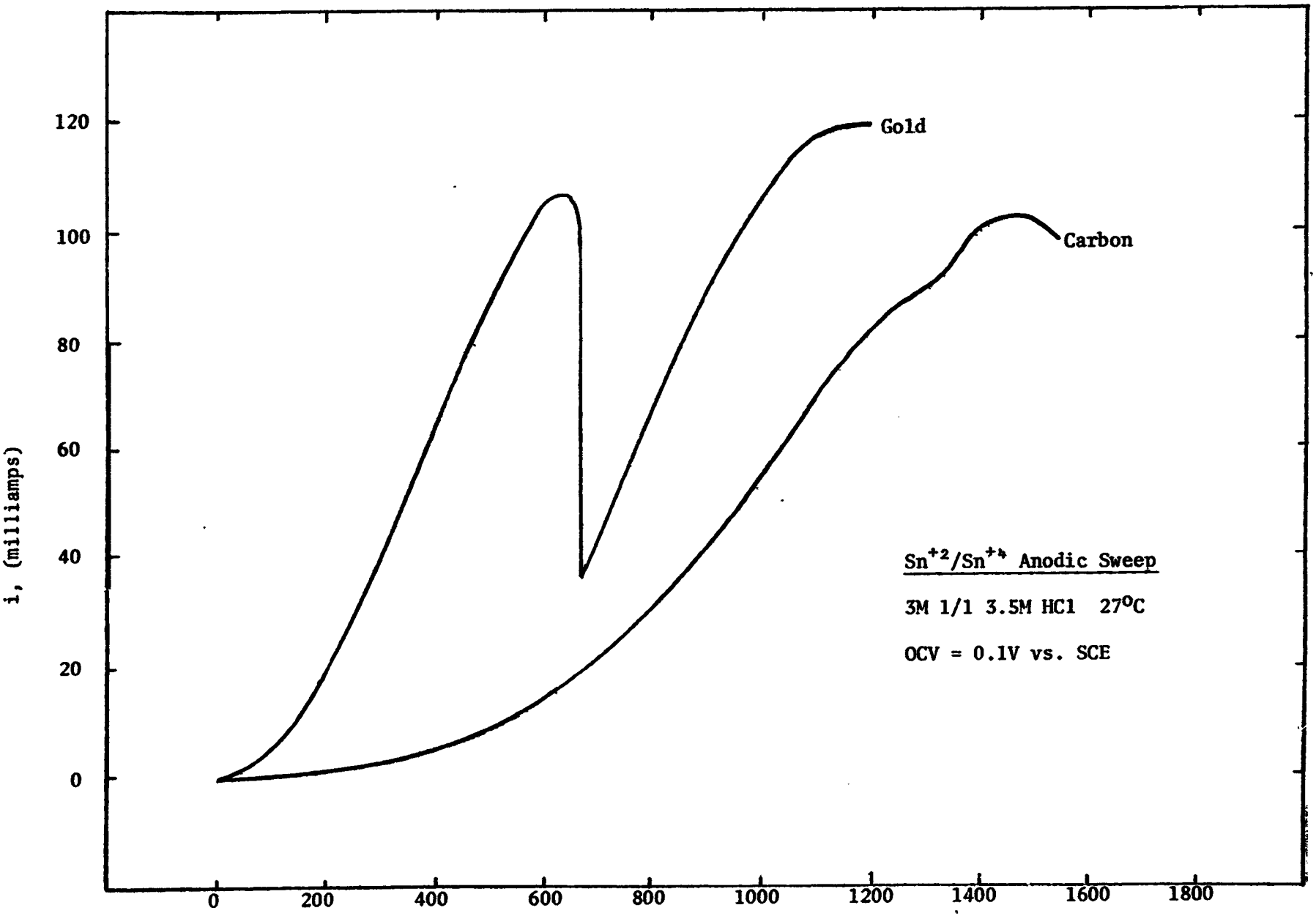

FIGURE 11. Typical curves obtained for Sn^{+2}/Sn^{+4} on gold and carbon electrodes

corrected using the equation*:

$$i_{corr} = i_{meas} / \left(1 - \frac{i_{meas}}{i_{L(a)}}\right) \qquad (6)$$

The exchange current densities, derived from plots of η_{corr} versus log i_{corr}, are shown in Table IX (open circuit potentials were erratic; E^o = -0.1V vs. SCE). The curves for carbon show two distinct slopes as reported by Lerner and Austin. The plots of the data on gold tend to show a continuous curve. For these reasons, exchange current densities shown in the table are very approximate.

c. Sb^{+3}/Sb^{+5} (3M HCl)

The five antimony couple compositions found to be soluble were all tested. A number of problems were encountered with this couple.

On gold, anodic limiting currents could not be measured due to the early onset of gold corrosion; this was not unexpected since the open circuit potential of the antimony couple was relatively high (~ 0.5 to 0.6V vs. SCE). Unambiguous limiting current data could not be obtained on carbon either; a curve that appeared to finally approach a current plateau was frequently followed by a negative peak in the current, as is shown in Figure 12.

Cathodic limiting currents could not be obtained either, on gold or carbon, due to a reaction occurring at a polarization of 0.2 to 0.5V, that deposited a brown, non-metallic residue on the surface of the electrode (Au and C). The deposited material could be stripped anodically. This observation is consistent with the solubility problems encountered with high Sb^{+3} concentrations (all 10:1 ratios were insoluble).

*The second term in the denominator of equation (2) is dropped because of the high polarization used.

TABLE IX. EXCHANGE CURRENT DENSITY, -log i_o (A/cm^2)

Sn^{+2}/Sn^{+4} (3.5 N HCl)

Total Concentration	Red/Oxid.	27°C Gold	27°C Carbon	50°C Gold	50°C Carbon
1M	1/10	3.0	4.5	2.2	4.2
	1/1	3.7	5.5	3.0	5.2
	10/1		4.7	3.4	
3M	1/10	2.2	5.4	1.7	5.2
	1/1	3.5	5.0	2.7	5.2
	10/1	4.4	4.8		6.7

NOTE: The exchange current values for the Sn^{+2}/Sn^{+4} couple are tentative. There is considerable uncertainty because of (a) lack of well defined cathodic iE-curve; (b) existence of one or more linearity breaks in the anodic log i_{corr} vs. η curve; and (c) because irreproducibility of the open circuit potential. The values tabulated here correspond to linear section in the anodic log i-η curve which extends only to η = 100 mV for gold and η = 300 mV for carbon.

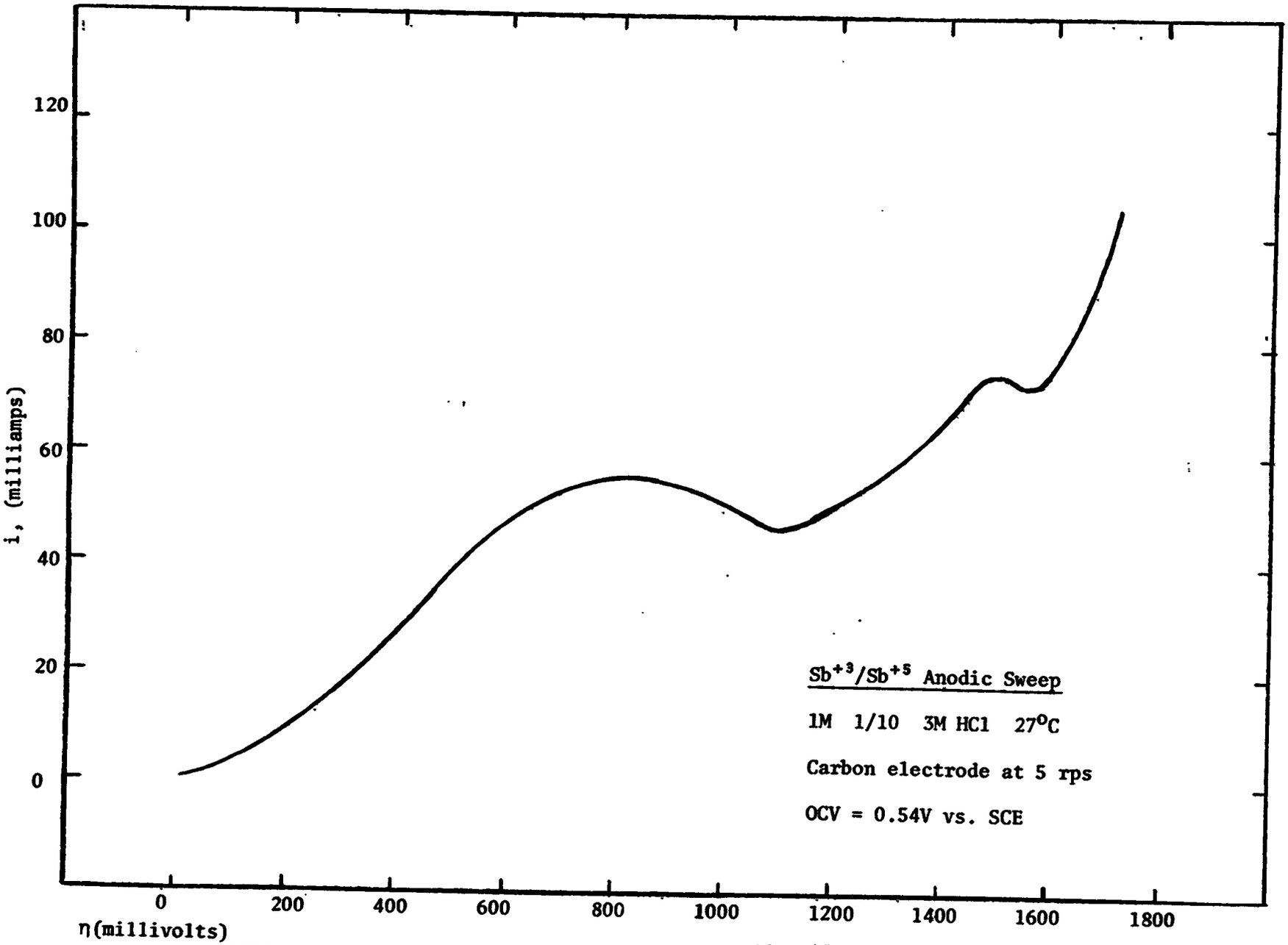

FIGURE 12. Typical I-E curve obtained with Sb^{+3}/Sb^{+5} on a carbon electrode.

Exchange current densities for this couple were estimated from the slope of the curve η versus i, at low polarization using the equation (5). The exchange current densities derived in this manner, are shown in Table X (open circuit potentials were erratic, E^o = 0.51 vs. SCE).

d. Ti^{+3}/Ti^{IV} (6M HCl)

Polarization data and limiting currents were obtained for the six soluble compositions of this couple. The reaction was quite reversible. The anodic data was generally good with stable limiting currents and no evidence of secondary reactions. The cathodic data was somewhat less straightforward, especially on carbon; sometimes several cathodic current plateaus were observed, or no distinct plateau. Additionally, the cathodic polarization measurements (steady state current at controlled potential) were subject to some drifting, particularly for the 1:10 ratios (high Ti^{IV} concentrations). There may have been a deposition reaction occurring since the gold electrode was sometimes observed to have a deposit on the surface after a cathodic sweep. This may have been due to generation of a high local concentration of Ti^{+3}, the product of the cathodic reaction, which was insoluble at some level below $\sim$ 4M.

Exchange current densities were derived from plots of η_{corr} versus log i_{corr}, using both anodic and cathodic data, using Equation (2). Exchange current densities and open circuit potentials are shown in Table XI.

e. $Cu(NH_3)_2^{+1}/Cu(NH_3)_4^{+2}$ (1M NaCl + 0.01M NaOH)

Four compositions of this couple were tested. In preliminary testing of this couple, it was found that precipitation of

TABLE X. EXCHANGE CURRENT DENSITY, -log i_o (A/cm^2)

Sb^{+3}/Sb^{+5} (3N HCl)

Total Concentration	Red/Oxid.	27°C Gold	27°C Carbon	50°C Gold	50°C Carbon
1M	1/10	3.3	4.0	2.8	2.8
	1/1	4.0	4.0	3.5	2.7
	10/1 (insol.)				
3M	1/10	3.0	4.0	2.4	2.9
	1/1	3.3	3.5	2.6	2.8
	10/1 (insol.)				
4M	1/10 (insol.)				
	1/1	3.5	4.3	2.7	3.3
	10/1 (insol.)				

TABLE XI. EXCHANGE CURRENT DENSITY, $-\log i_o$ (A/cm^2)

Ti^{+3}/Ti^{IV} (6N HCl)

Total Concentration	Red/Oxid.	27°C Gold	27°C Carbon	50°C Gold	50°C Carbon
1M	1/10	2.0	3.7-3.2	2.0-1.5	3.7-3.3
	1/1	1.9-1.7	3.7-3.3	1.3	3.0-2.4
	10/1	2.2-1.6	4.5	1.5	4.1
3M	1/10	1.7-1.4	3.4-2.2	1.7-1.2	3.4-2.0
	1/1	1.5-1.2	2.4-2.0	1.1-0.5	2.3-2.0
	10/1	2.4-2.3	3.5-3.2	2.0-1.3	3.3-2.7

OPEN CIRCUIT VALUES Ti^{+3}/Ti^{IV} (mV vs. SCE)

Total Concentration	Red/Oxid.	27°C Gold	27°C Carbon	50°C Gold	50°C Carbon
1M	1/10	28	51	51	49
	1/1	-34	-37	-19	-22
	10/1	-109	-100	-107	-110
3M	1/10	54	49	54	59
	1/1	-29	-26	-25	-22
	10/1	-94	-92	-92	-90

copper was occurring during the course of testing, apparently due to the loss of ammonia. This may have been due to the change in the complexing number in going from the reduced to the oxidized form. To eliminate this problem, ammonium hydroxide solution was substituted for the water in the N_2 presaturator. This was quite effective in preventing precipitation, and all four compositions were tested in this way.

This couple appeared to be quite reversible and showed fairly high limiting currents. A practical limitation may arise from the relative insolubility at the 10:1 redox composition. However, a 1M 5:1 composition was found to be soluble and was tested in place of the 10:1 composition.

Copper plating occurred at -400 to -500 mV vs. SCE, and this prevented measurement of a cathodic limiting current in some cases.

Exchange currents were derived from plots of η_{corr} versus log i_{corr}. The measured anodic current data was corrected according to Equation (6). For verification, a second correction was made using the complete correction of Equation (2) to correct for the back reaction at low polarization, in which a value for $i_{L(c)}$ (the cathodic limiting current, which was not measured) was calculated, according to the concentration ratio, from the measured anodic limiting current. These values extended the straight line portion of the curve to low values of current density in good agreement with the first correction. The exchange current densities for $Cu(NH_3)_2^{+1}/Cu(NH_3)_4^{+2}$ are presented in Table XII. Open circuit values for this couple are shown in Table XXXI of Section II (E^o = -0.25 vs. SCE).

f. Cr^{+2}/Cr^{+3} (1M HCl)

As discussed above, two compositions of this couple were partially soluble; an approximate 1:10 1M composition (0.08M Cr^{+2}/0.9M Cr^{+3}), and an approximate 1:1 1M composition (0.33M Cr^{+2}/0.5M Cr^{+2}). Limiting

TABLE XII. EXCHANGE CURRENT DENSITY, -log i_o (A/cm^2)

$Cu(NH_3)_2^{+1}/Cu(NH_3)_4^{+2}$ (1M NaCl + 0.01 NaOH)

Total Concentration	Red/Oxid.	27°C Gold	27°C Carbon	50°C Gold	50°C Carbon
1M	1/10	2.2	2.0	1.5	2.4
1M	1/1	1.6	2.0-1.6	1.6-1.4	1.5
	10/1	1.1	1.3	1.8	2.0-1.5
3M	1/10	1.4	1.8	1.7-1.3	1.6-1.2
	1/1	1.4	1.5	1.7-1.6	1.6-1.3
	10/1 (insol.)				

currents for the two compositions of this couple could not be measured cathodically due to hydrogen evolution (E^o = -0.65V vs. SCE), and anodic limiting currents tended to be unstable and not reproducible. Exchange current densities were estimated from the slope of the curve η versus i, at low polarization, using Equation (3).

The exchange current densities for Cr^{+2}/Cr^{+3} are shown in Table XIII. Open circuit values for this couple are shown in Table XXXI of Section II.

g. Br^-/Br_3^- (NaBr)

Six compositions of this couple were prepared and exchange current densities were measured. Due to gold corrosion and interfering anodic reactions at the high potential of this couple, measurements with this couple were limited to cathodic polarization curves on carbon at 27°C. Measurements at 50°C were not taken due to the unavailability of bromine solubility data at this temperature (excessive bromine vapor was observed on attempting to heat to 50°C). This couple is highly reversible. The method used for the determination of exchange currents was similar to that used for the $Cu(NH_3)_2^{+1}/Cu(NH_3)_4^{+2}$. The exchange current densities obtained and the open circuit potential values measured are shown in Table XIV.

TABLE XIII. EXCHANGE CURRENT DENSITY, -log i_o (A/cm^2)

Cr^{+2}/Cr^{+3} (1M HCl)

Total Concentration	Red/Oxid.	27°C Gold	27°C Carbon	50°C Gold	50°C Carbon
1M	∿ 1/10	2.7	4.3	2.8	4.2
	∿ 1/1	2.7	4.2	2.3	4.1

TABLE XIV. EXCHANGE CURRENT DENSITY, -log i_o (A/cm^2)

Br^-/Br_3^- (NaBr)

Total Br Conc. (g-atom/ℓ^{-1})	Br^-/Br_3^- Red/Oxid.	-log i_o at 27°C on carbon
2.1	0.3/0.6	2.2
2.1	0.9/0.4	2.5-2.2
2.1	1.5/0.2	3.0-2.7
9	0/3	2.0
9	3/2	2.1
9	6.3/0.9	2.2-2.0

OPEN CIRCUIT VALUES Br^-/Br_3^- (mV vs. SCE)

2.1	0.3/0.6	813
2.1	0.9/0.4	799
2.1	1.5/0.2	766
9	0/3	798
9	3/2	754
9	6.3/0.9	724

D. SUMMARY AND CONSLUSIONS

Solubility: In attempting to prepare the solutions suggested in the Work Statement of this Contract, solubility limitations have been established in a broad manner for the different redox couples studied.

The highest solubilities were obtained with the Sn^{+2}/Sn^{+4} couple, which is soluble (in 3.5N HCl) up to a total concentration of 5 molar at all the three studied redox ratios (1:10, 1:1 and 10:1). Solubility of up to 3M was obtained, at the same three redox ratios, with the Fe^{+2}/Fe^{+3} couple (in 1N HCl) and with the Ti^{+3}/Ti^{IV} (in 6N HCl). The Br^-/Br_3^- couple also shows high solubility, 9 Normal in total bromine, at moderate Br_2 partial pressure, but in order to keep this pressure low, only 2/3 of this bromine can be charged.

All the other couples showed limitations below a total concentration of 3 molar (the reduced species being the most difficult to dissolve). Thus, the Sb^{+3}/Sb^{+5} couple was soluble (in 3N HCl) up to 3M total concentration at the 1:10 and 1:1 ratio, but the 10:1 ratio could not be dissolved. The $Cu(NH_3)_2^{+1}/Cu(NH_3)_4^{+2}$ couple was soluble as a chloride (in 1M NaCl, 0.01M NaOH and 1 atm NH_3) at the 1:10, 1:1 and 5:1 ratios (but the 10:1 ratio could not be dissolved). At the 3 molar total concentration level this couple was still soluble at 1:10 and 1:1 ratios, but at this concentration the 5:1 ratio could not be dissolved. Chromous chloride, as obtained from different suppliers, was very difficult to dissolve (in contrast with published data); the highest solubility attained was 0.33M Cr^{+2}/0.5M Cr^{+3}. The low solubility observed may have been due to the formation of oxychloride intermediates. The chromo/chromi cyanide couple presented even more difficulties and no suitable solution for these tests ($\geq$ 1 molar) could be prepared.

Conductivity: The specific conductance of the various redox solutions are presented in Tables I to VII and Figures 4 to 10.

Within the solutions based on HCl, conductance increases as would be expected with increasing HCl concentration, but it decreases with increasing total concentration of redox reactants, probably because of increasing Cl^- complexing and viscosity. In the case of Fe^{+2}/Fe^{+3}, Sn^{+2}/Sn^{+4} and Sb^{+3}/Sb^{+5} conductivity increases with increasing redox ratio; suggesting less Cl^- complexing by the reduced species. (Such effect is very pronounced with the Sn^{+2}/Sn^{+4} and Sb^{+3}/Sb^{+5} couples). Ti^{+3}/Ti^{IV} and Cr^{+2}/Cr^{+3}, on the other hand, show a decrease of conductivity with increasing degree of reduction.

The $Cu(NH_3)_2^{+1}/Cu(NH_3)_4^{+2}$ couple shows a peculiar effect of redox ratio on conductivity. This decreases when redox ratio is changed from 1:10 to 1:1 and then increases by almost an order of magnitude when changing from 1:1 to 10:1. (An explanation for this behavior is still lacking.)

Finally, the conductivity of the bromine couple increases as one would expect when the redox ratio increases (more ionic species present).

Viscosity: Viscosity data is also presented in Tables I to VII and Figures 4 to 10. In all cases viscosity for each couple increases with increasing total redox couple concentration. With the exception of the concentrated Br^-/Br_3^- couple, the viscosity of solutions of a given couple is affected by concentration (total concentration and redox ratio) in the same direction as is conductance. In the case of 5M Sn^{+2}/Sn^{+4} solutions, the effect of redox ratio on viscosity is very large, decreasing almost by a factor of 5 (at 27°C) when the redox ratio changes from 1:10 to 10:1.

Exchange Current: A summary of exchange currents under similar conditions for the different couples is shown in Table XIV.B. The table shows also the varying effect of electrode material (carbon vs. gold) on exchange current.

Of the positive electrode couples, Fe^{+2}/Fe^{+3} has the highest exchange current and is the best behaved. The Br^-/Br_3^- couple has an almost equally high exchange current and a higher electrode potential (about 300 mV higher than for Fe^{+2}/Fe^{+3}). Problems with this couple are its corrosivity (related to the high electrode potential) and the finite bromine vapor pressure, especially high at 50°C. The Sb^{+3}/Sb^{+5} couple has an exchange current about two orders of magnitude lower than both the iron and bromine couples. It shows also side reactions (precipitation) at potentials removed from the practical operating potential. It is not clear to what extent these problems will be significant with porous electrodes at operating, practical potential (because of the higher current densities involved).

For the testing in redox flow reactors, the Fe^{+2}/Fe^{+3} and Br^-/Br_3^- couples were selected; the first to serve as a baseline and the second because of its promise.

Of the negative electrode couples, the Ti^{+3}/Ti^{IV} couple is the best behaved and has a very high exchange current on gold (on carbon its exchange current density is 30 to 75 times smaller). The $Cu(NH_3)_2^{+1}/Cu(NH_3)_4^{+2}$ has a high exchange current, both on carbon and gold, and has a favorable redox potential. The problems with this couple are the limited solubility of the reduced form (discussed above) and the limited range of cathodic polarization before copper deposition. The Cr^{+2}/Cr^{+3} couple shows reasonable exchange current especially on gold, but it caused considerable

problems during this investigation regarding solubility (especially of the reduced species) and hydrogen evolution. The Sn^{+2}/Sn^{+4} couple is the most irreversible of all the studied couples and has considerable asymmetry between anodic and cathodic direction. It shows a small kinetically controlled limiting current (or current peak) in the cathodic direction and distinct change of mechanism in the anodic direction. The measured exchange currents of the Sn^{+2}/Sn^{+4} couple are erratic for these reasons. In spite of the uncertainty in the data, the exchange current densities obtained on gold are clearly higher than the exchange current densities obtained on carbon by one or two orders of magnitude.

For studies in redox flow reactors, the $Cu(NH_3)_2^{+1}/Cu(NH_3)_4^{+2}$ and the Cr^{+2}/Cr^{+3} couples were chosen.

A discussion of the effect of concentration on exchange current has to consider that the effects are, in general, small (see discussion of simple theoretical consideration in Appendix II), and are masked to some extent, by the lack of precision intrinsic to such a broad screening program.

The exchange current of the Fe^{+2}/Fe^{+3} couple shows a dependence on redox ratio for all studied conditions as follows:

$$i_{o(1:1)} > i_{o(10:1)} > i_{o(1:10)}$$

Increasing total concentration of Fe increases the measured exchange current, but only weakly. The exchange current of the Ti^{+3}/Ti^{IV} couple shows a clear dependence on Redox ratio as follows:

$$i_{o(1:1)} > i_{o(1:10)} > i_{o(10:1)}$$

With this couple there is a clear increase of exchange current with concentration. The exchange current of the bromine couple increases slightly with increasing

total bromine concentration and appears to decrease slightly with increasing degree of reduction. For the Cr^{+2}/Cr^{+3} there appears to be very little effect of redox ratio (in three out of four cases) on exchange current.

The effect of concentration on the exchange current of the other couples (Sb^{+3}/Sb^{+5}; $Cu(NH_3)_2^{+1}/Cu(NH_3)_4^{+2}$ and Sn^{+2}/Sn^{+4}) appears less clear.

TABLE XIV.B

COMPARISON OF EXCHANGE CURRENT DENSITIES OF ...

DIFFERENT COUPLES UNDER SIMILAR CONDITIONS

Total concentration = 1M; Redox ratio = 1:1; Temperature = 27°C

	$-\log i_o$ (A/cm^2)	
Positive Electrode Couples	**Gold Electrode**	**Carbon Electrode**
Fe^{+2}/Fe^{+3}	1.2	2.0
Br^-/Br_3^- *	(not tested)	2.2-2.5
Sb^{+3}/Sb^{+5}	4.0	4.0
Negative Electrode Couples		
$Cu(NH_3)_2^{+1}/Cu(NH_3)_4^{+2}$	1.6	1.6-2.0
Ti^{+3}/Ti^{IV}	1.8	3.3-3.7
Cr^{+2}/Cr^{+3}	2.7	4.2
Sn^{+2}/Sn^{+4}	3.7	5.5

*2.1N in total Br, Red/Ox ratio = 2.25

II. TASK II - SECOND STAGE OF SCREENING OF REDOX COUPLES

A. INTRODUCTION

The second phase of this program involved the attainment of three objectives: (1) to improve the performance of small redox flow reactors by testing, under flow conditions, a number of different electrode materials and structures; (2) to test the suitability, under flow conditions, of four redox couples selected in Phase I; (3) to compare with the Fe^{+2}/Fe^{+3} couple (the base line), a number of couples used in flow cells with different electrodes.

The approach for this task was a purely empirical one, aimed primarily at testing a large variety of electrode materials and structures. A systematic study using electrochemical reactor theory is to be performed at a later date.

The couples chosen for study in Phase II were the following:

1. Fe^{+2}/Fe^{+3}

This is a well understood and well behaved couple. It has been studied at NASA-Lewis and, consequently, it was useful as a base line of performance, particularly for positive electrode couples.

2. Br^-/Br_3^-

The choice of this couple was based on its very high OCV and on the high exchange current densities observed in Phase I. Although Br_2 is very corrosive, inexpensive graphite might be used for cell construction, with some limitations.

3. $Cu(NH_3)_2^{+1}/Cu(NH_3)_4^{+2}$

This couple was chosen because RDE measurements showed that it was quite reversible, and the OCV of the couple is well placed for

operation as a negative electrode couple. Exchange current densities were quite high on both gold and carbon.

4. Cr^{+2}/Cr^{+3}

This couple, in limited testing, showed moderate exchange current densities, has a quite negative OCV, and it has been suggested elsewhere as the negative electrode redox couple for an all chromium redox cell. Although many problems were encountered in Phase I regarding the solubility of the $CrCl_2$, it was hoped that these problems had to do with the formation of oxychlorides in the three different sources tried, and that electrochemically generating the chromous salt from the chromic salt might solve the problems.

B. ELECTROCHEMIAL PERFORMANCE MEASUREMENTS

1. Electrode Structures

During the course of this study, three broad types of electrode structures were considered:

a. Frontal Electrode Structures

This type of electrode was a porous open structure like screen or graphite paper. It was placed in contact with the ion exchange membrane, and the reactant-electrolyte flowed behind the electrode through a "pin" field in the back plate of the cell.

b. Recessed Electrode Structures

This type of electrode was either a non-porous sheet like platinized titanium sheet or a microporous structure like carbon or activated carbon. It was located against the back plate of the cell with coarse plastic screen between the electrode and the ion exchange membrane,

permitting reactant-electrolyte to flow in front of the electrode.

c. Cavity Filling Electrode Structures

A typical example of this structure is the woven graphite cloth used in NASA-Lewis experiments. This type of electrode filled the cavity and the reactant-electrolyte flowed through the structure.

2. Electrode Materials

The range of electrode materials to be studied in Task II was expanded somewhat in order to compensate for the smaller number of solutions tested in Task I due to solubility limits. Instead of using the same four electrodes for each of the four couples, we investigated a larger number of electrodes, selecting for each redox couple tested the four electrodes which appeared most suited for the specific couple. This allowed us to obtain more useful and relevant information in a selective manner. Some of these electrode materials were purchased directly and used without modification, such as Pt screen*, Au screen, platinized titanium sheet, porous carbon block, and graphite cloth. Various other electrodes were prepared as described below:

a. Kreha Graphite Paper Stabilized With Teflon

Various concentrations of TFE in Kreha paper were tested for stability, wetting and electrical conductivity. A sample with 4.5 mg TFE/cm^2 appeared to have the best combination of these properties and was selected for testing.

b. Titanium Screen Activated With Ruthenium Oxide

Titanium screen was activated with RuO_2* according to

*For all electrodes involving the use of noble metals, it is intended that in the ultimate practical electrode the noble metal would be highly dispersed, at a very low loading (<< 1 mg/cm^2).

procedures described in the literature.[9] The method used was as follows: a piece of titanium screen was cleaned and degreased by refluxing in isopropyl alcohol vapor; a solution of 0.1M $RuCl_3 \cdot xH_2O$ (Ventron) was prepared in 20% HCl. The degreased screen was dipped in the $RuCl_3$ solution, dried at 110°C for five minutes, and baked in a tube furnace at 350°C for ten minutes under a forced air atmosphere. This procedure was repeated six times and after the final coating, the screen was heated to 450°C under forced air for one hour. (This is the procedure given by Yeager, et al.)[9] The resulting electrode had a RuO_2 loading of $\sim$ 4.5 mg/cm^2.

c. Screen With TFE-Bonded Highly Dispersed Carbon

High surface area carbon (Vulcan XC-72) was bonded with Teflon to screen using standard electrode fabrication technology. Various substrate screens were used according to the application (gold plated tantalum for acid supporting electrolytes and pure gold grid in alkaline-NH_3 electrolytes). The Teflon level chosen was 20% (Dupont TFE-30 dispersion), which was adequate for electrode integrity without producing hydrophobicity. The loading was $\sim$5mg carbon/cm^2.

d. Screen With TFE-Bonded Au- or Pt-Activated Carbon

These electrodes were prepared in the same general manner as described above. The carbon was activated with either gold or platinum according to the following procedure to give noble metal loadings of $\sim$ 0.5 mg/cm^2: gold chloride or platinum chloride was reduced with formaldehyde according to the procedure of Giner, Parry and Smith[10] to produce a high surface area black; the noble metal blacks thus produced were combined with carbon and 20% Teflon to produce a dispersion of the metal over the surface of the carbon with loadings of 4.5 mg carbon/cm^2 and 0.5 mg noble metal/cm^2.

3. Flow Reactor Design

Two cells were fabricated from Noryl (polyphenylene oxide), with movable graphite contact blocks, as shown in Figure 13. Two variations of the contact block were made, a flat surface and a "pin" field surface. The dimensions of the active electrode surface area were 2.5 cm x 4 cm (10 cm^2). The cell could either be operated in the frontal electrode position, allowing electrolyte to flow between the electrode and the "pin" field back plate of the cell, or in the recessed electrode position against the flat back plate allowing electrolyte to flow between the electrode and the ion exchange membrane.

The electrolyte gap, i.e. distance between the back plate or flat-electrode and separator was 0.5 mm for graphite cloth and electrodes in the recessed location, and 2.5 mm for electrodes in frontal location. The ion exchange membranes used were Ionics 103-QZL-183 for Fe^{+2}/Fe^{+3} and Cr^{+2}/Cr^{+3}, Nafion-120 for Br^-/Br_3^- and $Cu(NH_3)_2^{+1}/Cu(NH_3)_4^{+2}$. The cell was thermally insulated, and the electrolyte was preheated in reservoirs of 2000 cc capacity. The temperature of the cell was monitored as the electrolyte flowed through. The cells were operated at 27°C and 50°C, except Br^-/Br_3^- which was operated only at 27°C.

Flow of electrolyte through the cell from the reservoirs was controlled by variable flow pumps of up to 600 cc/min capacity. A flow of 20 cc/min was used for the graphite cloth (cavity filling structure). A single flow rate (300 cc/min) was used for all other tests (electrodes in the frontal or recessed positions). At this flow rate the overall concentration change during an anodic or cathodic segment of a run was calculated to be under 1%, and the entry-to-exit change across the cell should have been between 2 and 5% and not more than $\sim$ 8% in the worst case (400 mA/cm^2 and $\sim$ 0.1 M/ℓ of reactant).

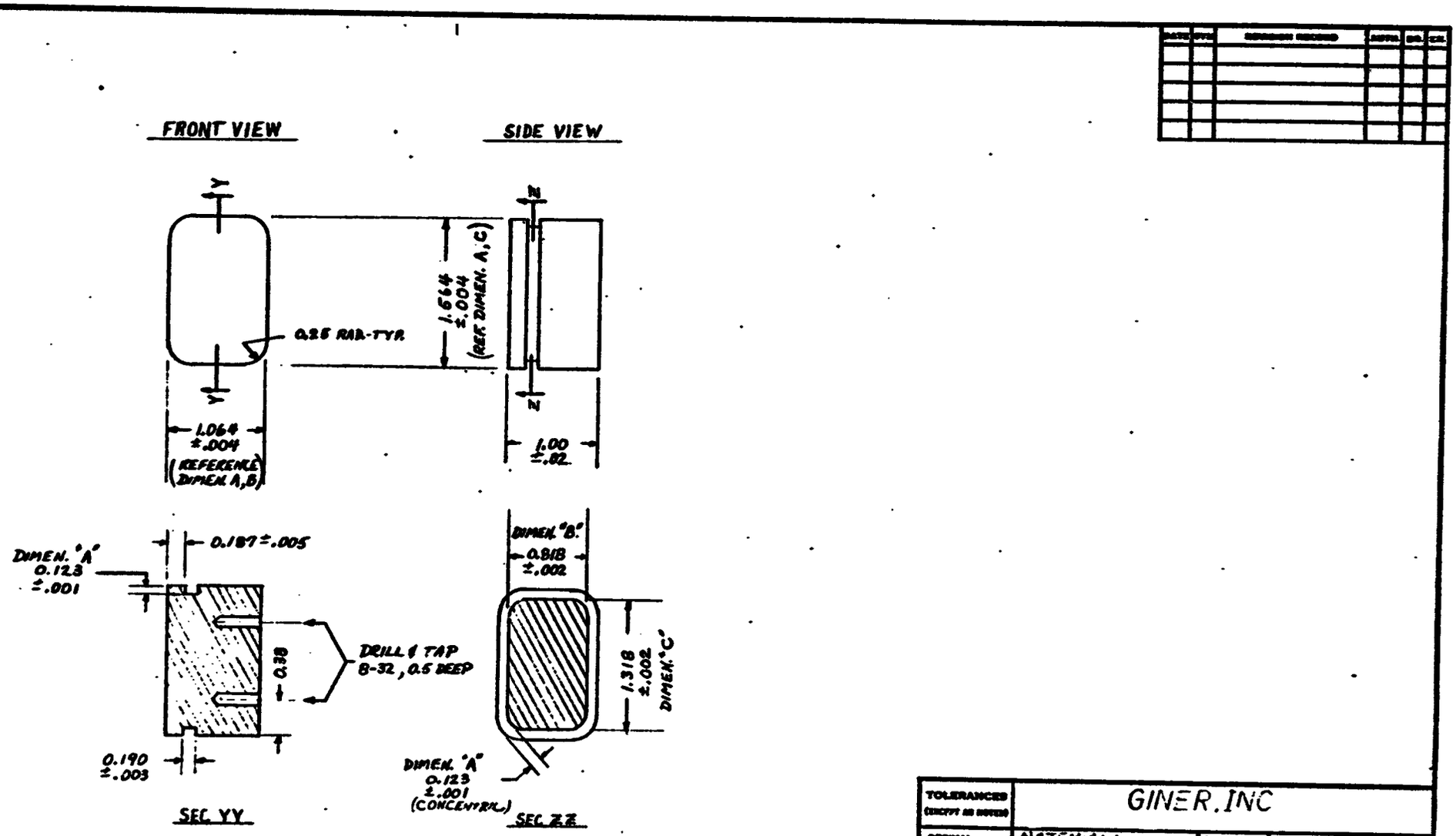

Figure 13a. Redox Cell.

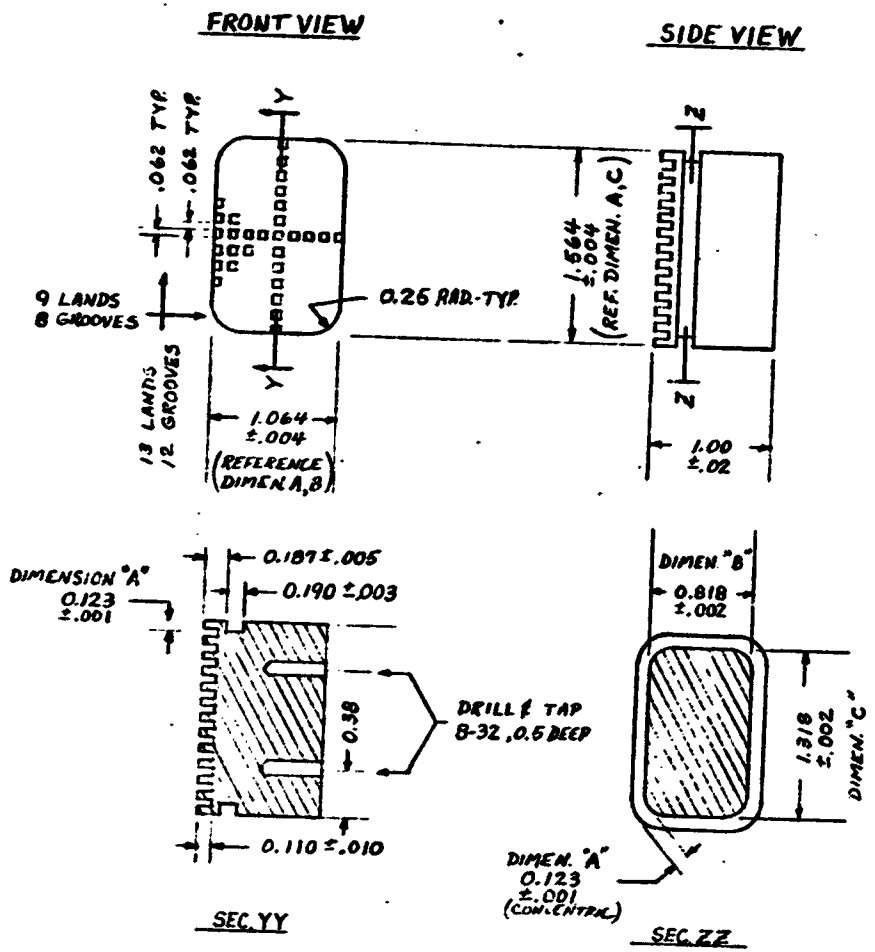

DATE	BY	REVISION RECORD	AUTH.	DR.	CK.

-09-

TOLERANCES (UNLESS OTHERWISE NOTED)	GINER, INC		
DECIMAL ±	MATERIAL: Hi-DENSITY GRAPHITE ATJ OR EQUIV.	SCALE 1mil = 1in	DRAWN BY
FRACTIONAL ±	TITLE REDOX CELL CONTACT BLOCK B		APPROVED BY
ANGULAR ! ±	DATE 3/16/76	DRAWING NUMBER G/N-06	

Figure 13b. Redox Cell.

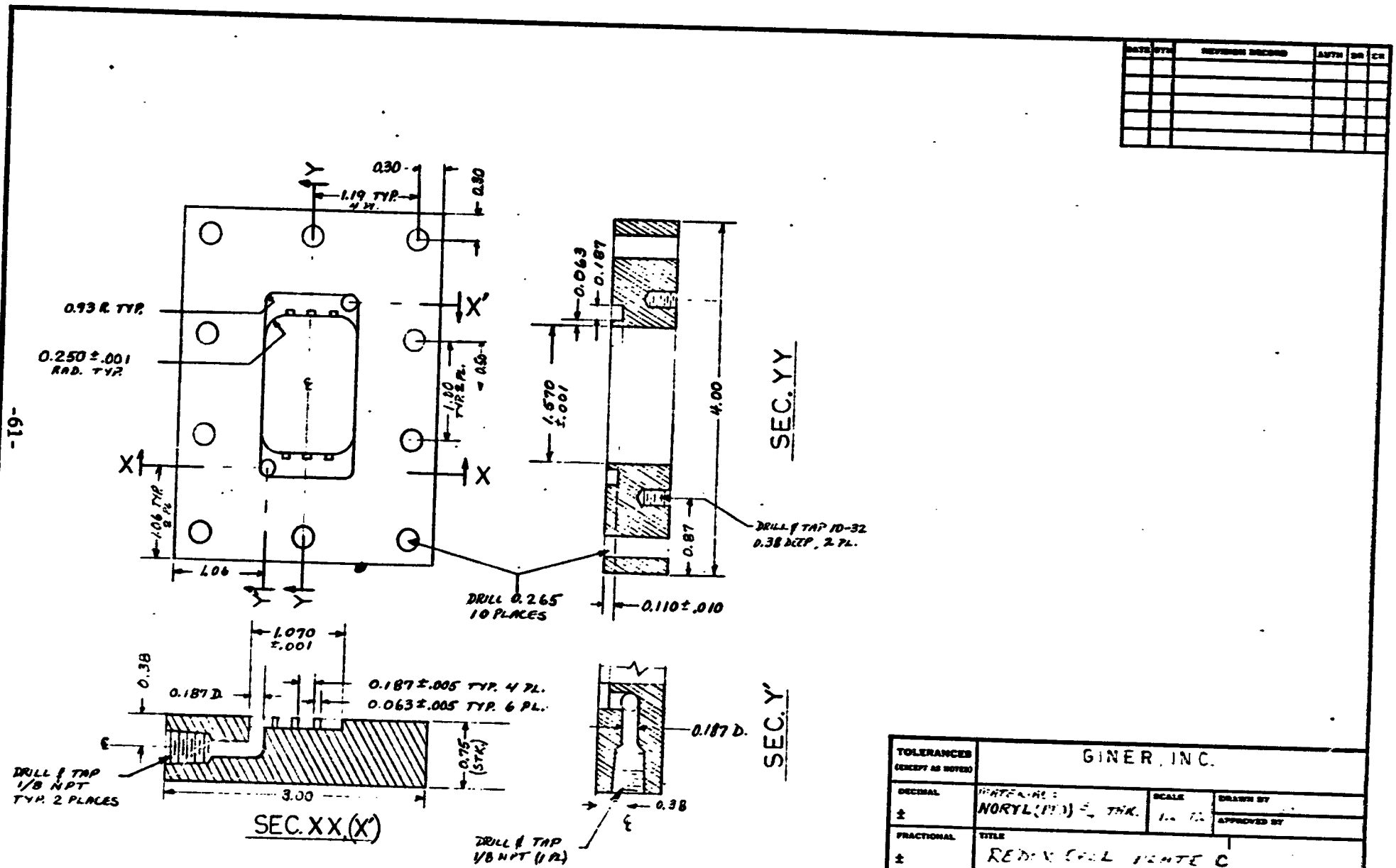

Figure 13c. Redox Cell.

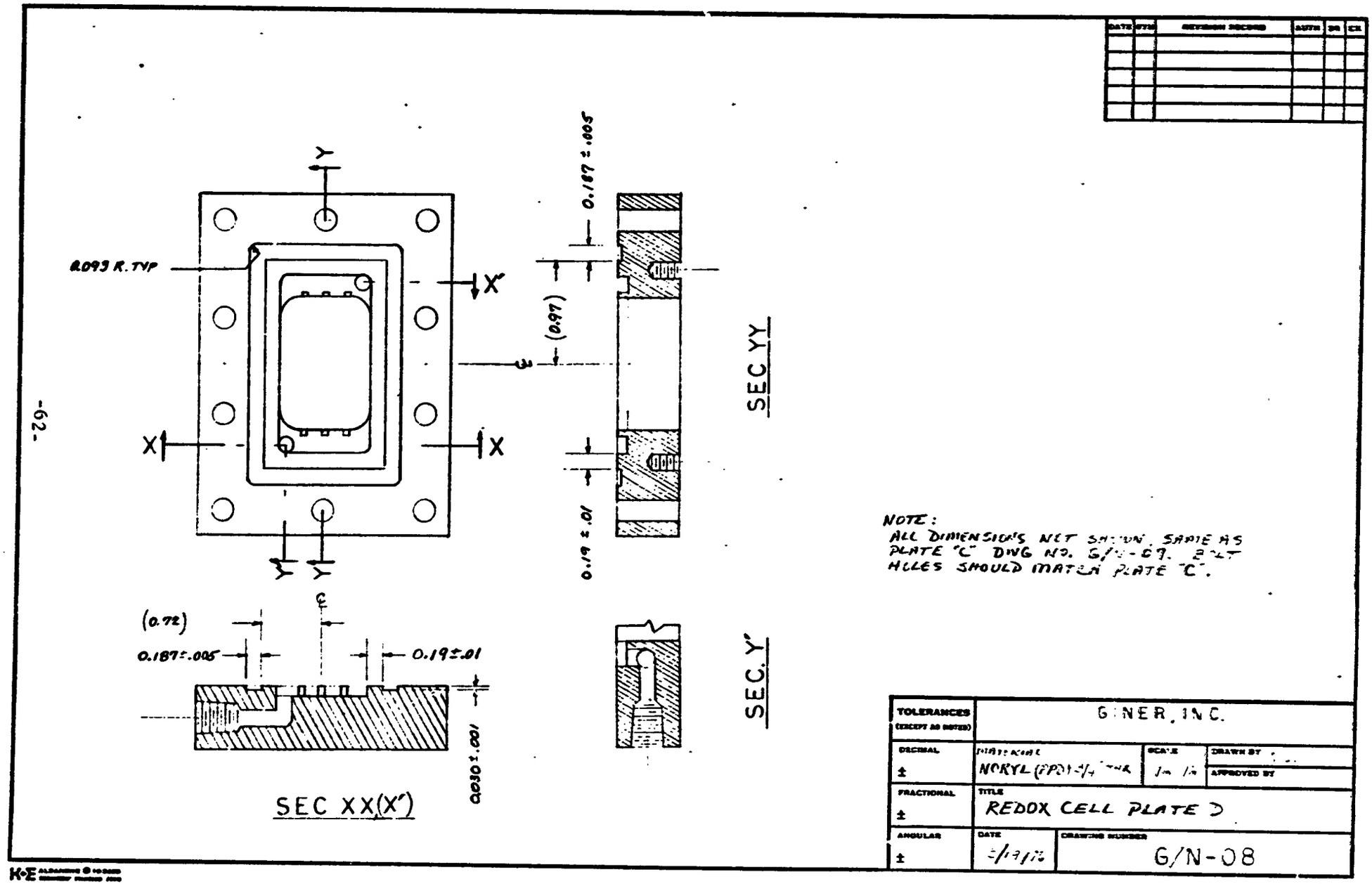

Figure 13d. Redox Cell.

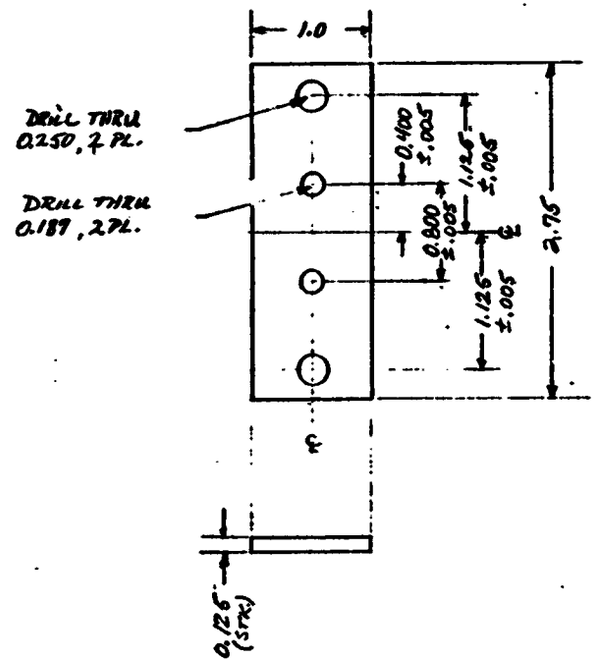

DATE	BY	REVISION RECORD	APPR.	DR	CK

TOLERANCES (EXCEPT AS NOTED)	GINER, INC.		
DECIMAL ±	MATERIAL: C.R. STEEL	SCALE 1 = 1½	DRAWN BY APPROVED BY
FRACTIONAL ±	TITLE: REDOX CELL PRESSURE PLATE		
ANGULAR ±	DATE 2/19/82	DRAWING NUMBER G/N-09	

H-E

Figure 13e. Redox Cell.

The flow rates appropriate for optimum power production are more difficult to determine. In this case the important parameter is the linear velocity, or the related Reynolds number. The linear velocity, for a flow rate of 120 cc/min and a cross section of 2.5 x 0.3 = 7.5 cm^2 is 2.67 cm/sec. For a liquid with a kinematic viscosity of 2 centipoise, flowing through a cell of cross section 2.5 x 0.3 cm (equivalent diameter = 0.54 cm), the Reynolds number is 72. If turbulence is not promoted, operation at this Reynolds number will result in a low mass transfer coefficient (or related Sherwood number). As a consequence, a higher flow rate would be required. Taking into consideration the results and equation of Leveque, Rousar, Newman and others, as discussed by Pickett and Stanmore,[11] it appears that flow rates 5 to 10 times higher would be required in order to obtain a sufficiently high mass transfer coefficient. Consequently, the cell was designed to promote some degree of turbulence in order to operate at somewhat lower flow rates.

4. Experimental Procedure

The electrochemical flow reactor was assembled with the appropriate membrane and electrodes and set up with a pump and reservoir connected to each electrode chamber. One of the four redox compositions being tested was pumped through the chamber containing one of the four electrode structures. The opposing side of the cell was operated as a counter electrode using an open electrode configuration (gold screen or graphite paper) in a frontal structure, and the same redox couple generally in a 1:1 ratio at 1 or 2M concentration. The flow rate on both sides was $\sim$ 300 cc/min, except for graphite cloth (20 cc/min). The reactor was designed to accommodate a reference electrode at the outlet on each side. After some initial testing using calomel electrodes at these locations, the reference in the counter electrode side was modified slightly to yield a more accurate measurement of the iR drop. A platinum

probe was placed behind and slightly below the center of the counter electrode, which was a porous frontal structure in all cases. A calomel electrode was placed at the test electrode side outlet as before (pressurized to prevent backflow through the junction). Open circuit was measured versus calomel then, and polarization was measured versus the platinum reference. Finally, the resistance was measured for the test electrode versus the platinum reference, using the current interrupter method, and this resistance was used to correct the polarization data. (Average open circuit voltages for all couples are shown in Table XXXI.)

Polarization curves were obtained in both the anodic and cathodic direction for each composition of each couple, each electrode and each temperature. The data was obtained by applying constant current in steps (1, 3, 6, 12, 25, 50, 100, 200 and 400 mA/cm^2, if possible) and monitoring the voltage change versus the Pt reference.

In general solutions were prepared in two redox ratios to represent an 86% charged condition and an 80% discharged condition. Two total concentrations were prepared for each couple whenever possible according to the solubility data obtained in Task I.

5. Results

a. Fe^{+2}/Fe^{+3} (1N HCl)

Four solutions of the Fe^{+2}/Fe^{+3} couple were prepared for testing in the fuel cell. These solutions were 1M and 3M $FeCl_2/FeCl_3$ with reduced/oxidized ratios of 1:6.25 for the "charged" state and 4:1 for the "discharged" state. There were no problems encountered in preparing these solutions. The counter electrode solution was a 2M Fe^{+2}/Fe^{+3} (1:1 reduced/oxidized) solution flowing at 300 cc/min on a gold screen electrode in a frontal structure. The membrane chosen for use with Fe^{+2}/Fe^{+3}

was 103-QZL-183. Initially, there were some problems with cracking of this membrane. This problem was eliminated by pretreating the membrane in 50°C in HCl for 1 hour.

i. Graphite Cloth (Base Line). Polarization measurements for the woven graphite cloth structure are listed in Table XV. The performance of this electrode was quite good, as found by NASA-Lewis in previous work.

ii. Pt Screen - Frontal Structure. This electrode was an 80 mesh Pt screen in a frontal structure. Polarization measurements are listed in Table XVI.

iii. Porous Carbon - Recessed Structure. This electrode consisted of 5 mg/cm^2 porous carbon (20% Teflon)on a 50 mesh gold plated tantalum screen. Polarization measurements are shown in Table XVII.

iv. Pt-Activated Carbon - Recessed Structure. This electrode consisted of 0.5 mg Pt/cm^2 on 4.5 mg carbon/cm^2 (20% TFE) on a gold grid support. Polarization measurements are shown in Table XVIII.

b. Br^-/Br_3^- (NaBr)

Four compositions of the Br^-/Br_3^- couple were prepared for testing. Two 9N solutions (86% charged and 20% charged) and two 3N solutions were prepared. The 9N, 20% charged solution was just at the solubility limit for the NaBr, so the solution concentration had to be shifted a little in the direction of Br_2. The flow rate for the experiments was 300 cc/min and the membrane was Nafion-120. The counter solution used in these experiments was a 7.5N 50% charged solution flowing over a graphite paper electrode in a frontal structure. This couple was operated only at 27°C.

TABLE XV Fe^{+2}/Fe^{+3} - POLARIZATION MEASUREMENTS

CONCENTRATION - 1M and 3M. $FeCl_2/FeCl_3$ (1M HCl)

ELECTRODE - Graphite Cloth Electrode "Within the Cavity" structure

FLOW RATE - 20 cc/min.

MEMBRANE - Ionics 103-QZL-183

Total Conc	Polarization (mV)			
1M	1/6.25 (Reduced/Oxidized)			
Current Den.	27°C		50°C	
mA/cm^2	Anodic	Cathodic	Anodic	Cathodic
1	6.			
3	6	1	1	2
6	7		3	4
12	7.	3	5	
25	12	11	14	13
50	18	26	29	34
100	448	81	232	87
200	908	116	878	109
400	3018	1396	3438	249

Total Conc	Polarization (mV)			
3M	1/6.25 (Reduced/Oxidized)			
Current Den.	27°C		50°C	
mA/cm^2	Anodic	Cathodic	Anodic	Cathodic
1	1	1	1	1
3	3	4	3	3
6	5	7	5	4
12	11	17	9	10
25	16	48	13	28
50		99	20	64
100	55	232	80	156
200	603	407	278	295
400	623	497		528

Total Conc	Polarization (mV)			
1M	4/1 (Reduced/Oxidized)			
Current Den.	27°C		50°C	
mA/cm^2	Anodic	Cathodic	Anodic	Cathodic
1			1	
3	1	2	2	1
6	2	5	3	2
12	4	11	6	6
25	8	24	10	12
50	13	47	18	22
100	40	121	48	74
200	268	148	177	123
400	1290	1430	560	1290

Total Conc	Polarization (mV)			
3M	4/1 (Reduced/Oxidized)			
Current Den.	27°C		50°C	
mA/cm^2	Anodic	Cathodic	Anodic	Cathodic
1		1		
3	1	3	1	
6	5	6		2
12	10	11	3	4
25	25	26	7	7
50	50	49	10	8
100	172	126	38	56
200	309	231	92	103
400	529	1431	357	1654

TABLE XVI Fe^{+2}/Fe^{+3} POLARIZATION MEASUREMENTS

CONCENTRATION - 1M and 3M $FeCl_2/FeCl_3$ (1N HCl)

ELECTRODE - Pt screen - frontal structure

FLOW RATE - 300 cc/min.

MEMBRANE - Ionics 103-QZL-183

Total Conc	Polarization (mV)			
1M	1/6.25 (Reduced/Oxidized)			
Current Den.	27°C		50°C	
mA/cm^2	Anodic	Cathodic	Anodic	Cathodic
1	2	2		
3	6	8	1	1
6	14	16	5	6
12	28	31	12	16
25	60	63	29	33
50	126	122	62	65
100	276	234	132	131
200	815	436	272	253
400	1435	812	683	497

Total Conc	Polarization (mV)			
3M	1/6.25 (Reduced/Oxidized)			
Current Den.	27°C		50°C	
mA/cm^2	Anodic	Cathodic	Anodic	Cathodic
1	4	4		
3	12	13	3	4
6	25	25	9	11
12	50	52	23	25
25	106	109	51	50
50	217	217	106	106
100	481	435	226	226
200	1239	812	495	426
400			1215	898

Total Conc	Polarization (mV)			
1M	4/1 (Reduced/Oxidized)			
Current Den.	27°C		50°C	
mA/cm^2	Anodic	Cathodic	Anodic	Cathodic
1	2	2		
3	7	5	2	2
6	13	11	5	5
12	25	23	14	12
25	54	49	30	27
50	101	97	59	54
100	205	193	122	113
200	403	441	245	222
400	758	1444	494	476

Total Conc	Polarization (mV)			
3M	4/1 (Reduced/Oxidized)			
Current Den.	27°C		50°C	
mA/cm^2	Anodic	Cathodic	Anodic	Cathodic
1	2	3	1	2
3	8	8	3	5
6	16	17	7	10
12	35	34	15	19
25	74	70	34	38
50	150	135	73	73
100	302	274	150	153
200	591	536	308	303
400			628	635

TABLE XVII Fe^{+2}/Fe^{+3} - POLARIZATION MEASUREMENTS

CONCENTRATION - 1M and 3M $FeCl_2/FeCl_3$ (1N HCl)

ELECTRODE - 5 mg/cm^2 Vulcan Carbon (20% TFE) on gold plated - tantalum screen - recessed structure

FLOW RATE - 300 cc/min.

MEMBRANE - Ionics 103-QZL-183

Total Conc	Polarization (mV)			
1M	1/0.25 (Reduced/Oxidized)			
Current Den.	27°C		50°C	
mA/cm^2	Anodic	Cathodic	Anodic	Cathodic
1	1	3	2	1
3	4	4	8	5
6	7	9	17	6
12	16	18	36	12
25	35	40	77	26
50	74	83	152	37
100	173	193	207	117
200	585	525	421	332
400		925	941	939

Total Conc	Polarization (mV)			
3M	1/6.25 (Reduced/Oxidized)			
Current Den.	27°C		50°C	
mA/cm^2	Anodic	Cathodic	Anodic	Cathodic
1	4	3	3	3
3	10	11	6	6
6	20	24	12	12
12	41	49	23	26
25	80	104	42	57
50	173	192	96	119
100	445	358	120	295
200	972	748	393	592
400				602

Total Conc	Polarization (mV)			
1M	4/1 (Reduced/Oxidized)			
Current Den.	27°C		50°C	
mA/cm^2	Anodic	Cathodic	Anodic	Cathodic
1		1	1	1
3	2	2	2	2
6	3	6	3	4
12	6	13	6	10
25	12	31	15	21
50	24	67	30	42
100	59	149	66	84
200	188	557	146	255
400	993	1597	761	1259

Total Conc	Polarization (mV)			
3M	4/1 (Reduced/Oxidized)			
Current Den.	27°C		50°C	
mA/cm^2	Anodic	Cathodic	Anodic	Cathodic
1	8	6	1	
3	16	13		
6	40	20	2	1
12	90	37	4	4
25	187	73	7	9
50	357	151	13	20
100	686	671	30	75
200	1075	1816	58	182
400	1495		162	

TABLE XVIII Fe^{+2}/Fe^{+3} - POLARIZATION MEASUREMENTS

CONCENTRATION - 1M and 3M $FeCl_2/FeCl_3$ (1N HCl)

ELECTRODE - 0.5 mg Pt/cm^2 on 4.5 mg Vulcan Carbon/cm^2 (20% TFE) on gold screen - recessed structure

FLOW RATE - 300 cc/min.

MEMBRANE - Ionics 103-QZL-183

Total Conc	Polarization (mV)			
1M	1/6.25 (Reduced/Oxidized)			
Current Den.	27°C		50°C	
mA/cm^2	Anodic	Cathodic	Anodic	Cathodic
1	1	1	1	1
3		3	2	3
6	2	5	4	4
12	3	11	8	10
25	10	24	17	20
50	24	43	34	38
100	167	101	105	80
200	676	323	200	168
400	816	864	785	343

Total Conc	Polarization (mV)			
3M	1/6.25 (Reduced/Oxidized)			
Current Den.	27°C		50°C	
mA/cm^2	Anodic	Cathodic	Anodic	Cathodic
1	1	2	1	3
3		4	3	5
6	2	6	5	7
12	5	14	8	15
25	14	24	18	29
50	27	34	35	48
100	168	148	92	186
200	353	587	194	303
400	553	897	474	683

Total Conc	Polarization (mV)			
1M	4/1 (Reduced/Oxidized)			
Current Den.	27°C		50°C	
mA/cm^2	Anodic	Cathodic	Anodic	Cathodic
1	6	3	2	1
3	19	9	6	3
6	38	17	13	7
12	76	36	25	13
25	152	75	56	30
50	279	132	156	61
100	366	216	265	92
200	448	764	295	119
400	546	894	385	565

Total Conc	Polarization (mV)			
3M	4/1 (Reduced/Oxidized)			
Current Den.	27°C		50°C	
mA/cm^2	Anodic	Cathodic	Anodic	Cathodic
1	1	2		
3	2	6	2	1
6	6	9	2	2
12	8	20	2	6
25	18	40	6	15
50	38	71	12	33
100	99	213	101	41
200	223	1045		185
400	606	1525		608

i. Porous Carbon - Recessed Structure. This electrode was a piece of porous carbon 3 mm thick (Stackpole Carbon #PC-58, 45% porosity) used in a recessed structure. Polarization measurements are shown in Table XIX.

ii. Teflonated Graphite Paper - Frontal Structure. This electrode was graphite paper impregnated with 4.5 mg TFE/cm^2 in a frontal structure. Polarization measurements are shown in Table XX.

iii. Platinized Ti Sheet - Recessed Structure. This electrode was platinized Ti sheet in a recessed structure. The polarization measurements are shown in Table XXI.

iv. RuO_2/Ti - Frontal Structure. This electrode was a piece of Ti screen coated with 4.5 mg/cm^2 RuO_2, in a frontal structure. The polarization measurements are shown in Table XXII.

c. $Cu(NH_3)_2^{+1}/Cu(NH_3)_4^{+2}$ (1M NaCl + 0.01M NaOH)

Two solutions of $Cu(NH_3)_2^{+1}/Cu(NH_3)_4^{+2}$ (0.01M NaOH + 1M NaCl) were prepared for testing; 1M1:4 reduced/oxidized (discharged state) and 1M 5:1 reduced/oxidized (charged state). These solutions were prepared by adding stock solution of NH_4OH (28% NH_3) to the $CuCl_2$ salt, allowing the complex to form and deaerating the solution. CuCl was then added to this solution. No water was added so that the NH_3 concentration could be kept as high as possible. Also, during cell operation, the N_2 gas was saturated with NH_4OH (28% NH_3) before being passed through the electrolyte. However,

TABLE XIX Br^-/Br_3^- - POLARIZATION MEASUREMENTS

CONCENTRATION: 3N and 9N Br (NaBr)

ELECTRODE: Porous Carbon - Recessed Structure

FLOW RATE: 300 cc/min. MEMBRANE: Nafion-120

Total Conc	Polarization (mV)	
3N 1/6.25	(Reduced/Oxidized)	
Current Den.	27°C	
mA/cm^2	Anodic	Cathodic
1		
3	1	1
6	2	2
12	5	3
25	8	7
50	16	13
100	24	48
200		68
400		

Total Conc	Polarization (mV)	
9N-1/6.25	(Reduced/Oxidized)	
Current Den.	27°C	
mA/cm^2	Anodic	Cathodic
1	1	1
3	2	2
6	3	2
12	6	6
25	11	11
50	24	25
100	36	41
200	75	70
400		

Total Conc	Polarization (mV)	
3N-4/1	(Reduced/Oxidized)	
Current Den.	27°C	
mA/cm^2	Anodic	Cathodic
1	1	
3	3	2
6	8	5
12	13	10
25	23	20
50	37	39
100	70	77
200	83	151
400		

Total Conc	Polarization (mV)	
9N-4/1	(Reduced/Oxidized)	
Current Den.	27°C	
mA/cm^2	Anodic	Cathodic
1	1	1
3	3	3
6	4	6
12	5	11
25	20	23
50	45	33
100	165	38
200	304	
400		

TABLE XX Br^-/Br_3^- - POLARIZATION MEASUREMENTS

CONCENTRATION: 3N & 9N Br (NaBr)

ELECTRODE: Teflonated Graphite Paper (4.5 mg TFE/cm^2) - Frontal Structure

FLOW RATE: 300 cc/min. MEMBRANE: Nafion-120

Total Conc	Polarization (mV)	
3N -1/6.25	(Reduced/Oxidized)	
Current Den.	27°C	
mA/cm^2	Anodic	Cathodic
1	2	1
3	5	3
6	8	4
12	13	9
25	28	17
50	49	36
100	117	92
200		
400		

Total Conc	Polarization (mV)	
9N-1/6.25	(Reduced/Oxidized)	
Current Den.	27°C	
mA/cm^2	Anodic	Cathodic
1	2	2
3	3	3
6	5	5
12	7	10
25	16	21
50	28	37
100	38	81
200	59	117
400		

Total Conc	Polarization (mV)	
3N-4/1	(Reduced/Oxidized)	
Current Den.	27°C	
mA/cm^2	Anodic	Cathodic
1	1	5
3	2	6
6	4	8
12	10	13
25	20	25
50	35	43
100	63	92
200	83	147
400		

Total Conc	Polarization (mV)	
9N-4/1	(Reduced/Oxidized)	
Current Den.	27°C	
mA/cm^2	Anodic	Cathodic
1	2	4
3	3	10
6	4	17
12	7	33
25	23	58
50	52	91
100	120	97
200		181
400		

TABLE XXI Br^-/Br_3^- - POLARIZATION MEASUREMENTS

CONCENTRATION: 3N & 9N Br (NaBr)

ELECTRODE: Platinized Ti Sheet - Recessed Structure

FLOW RATE: 300 cc/min. MEMBRANE: Nafion-120

Total Conc	Polarization (mV)	
3N 1/6.25	(Reduced/Oxidized)	
Current Den.	27°C	
mA/cm^2	Anodic	Cathodic
1	6	1
3	16	2
6	31	4
12	52	7
25	92	16
50	142	43
100		95
200		619
400		

Total Conc	Polarization (mV)	
9N-1/6.25	(Reduced/Oxidized)	
Current Den.	27°C	
mA/cm^2	Anodic	Cathodic
1	2	1
3	5	3
6	9	5
12	18	6
25	32	21
50	51	25
100		27
200		111
400		

Total Conc	Polarization (mV)	
3N-4/1	(Reduced/Oxidized)	
Current Den.	27°C	
mA/cm^2	Anodic	Cathodic
1	5	5
3	14	6
6	26	10
12	48	18
25	85	35
50	144	58
100		227
200		332
400		

Total Conc	Polarization (mV)	
9N-4/1	(Reduced/Oxidized)	
Current Den.	27°C	
mA/cm^2	Anodic	Cathodic
1	4	4
3	18	17
6	21	18
12	41	33
25	85	61
50	155	100
100	377	111
200	604	150
400		

TABLE XXII Br^-/Br_3^- - POLARIZATION MEASUREMENTS

CONCENTRATION: 3N & 9N Br (NaBr)

ELECTRODE: 4.5 mg RuO_2 on Ti Screen - Frontal Structure

FLOW RATE: 300 cc/min. MEMBRANE: Nafion-120

Total Conc	Polarization (mV)	
3N-1/6.25	(Reduced/Oxidized)	
Current Den.	27°C	
mA/cm²	Anodic	Cathodic
1	1	4
3	4	9
6	8	11
12	18	19
25	31	33
50	57	61
100	100	136
200	116	204
400		

Total Conc	Polarization (mV)	
9N-1/6.25	(Reduced/Oxidized)	
Current Den.	27°C	
mA/cm²	Anodic	Cathodic
1	1	3
3	3	4
6	7	6
12	12	12
25	24	25
50	48	43
100	74	70
200	156	160
400		

Total Conc	Polarization (mV)	
3N-4/1	(Reduced/Oxidized)	
Current Den.	27°C	
mA/cm²	Anodic	Cathodic
1		1
3	3	4
6	5	5
12	11	12
25	22	27
50	42	54
100	83	123
200	111	185
400		

Total Conc	Polarization (mV)	
9N-4/1	(Reduced/Oxidized)	
Current Den.	27°C	
mA/cm²	Anodic	Cathodic
1	2	2
3	4	6
6	6	12
12	13	25
25	29	47
50	72	85
100	208	94
200	356	168
400		

even with this precaution, the 5:1 solution did not seem to be too stable. A brownish sludge formed on the walls of the reservoir and inside the electrode chamber during operation. The counter solution used for this couple was 1M 1:1 $Cu(NH_3)_2^{+1}/Cu(NH_3)_4^{+2}$ flowing at 300 cc/min on a Au screen. The membrane chosen for this couple was Nafion-120 because of the higher pH.

i. Au Screen - Frontal Structure. This electrode was a gold expanded mesh in a frontal structure. Polarization measurements for this structure, which gave the best performance, are shown in Table XXIII.

ii. Porous Carbon - Recessed Structure. This electrode consisted of 5 mg/cm^2 Vulcan carbon (20% Teflon as binder)on a gold grid support in a recessed structure. Results are shown in Table XXIV.

iii. Au-Activated Carbon - Frontal Structure. This electrode consisted of 4.5 mg/cm^2 Vulcan carbon (20% Teflon as binder) activated with 0.5 mg/cm^2 Au, on a gold grid support in a frontal structure. Results are shown in Table XXV.

iv. Au-Activated Carbon - Recessed Structure. This electrode consisted of 4.5 mg/cm^2 Vulcan carbon (20% Teflon as binder), activated with 0.5 mg/cm^2 Au, on a gold grid support in a recessed structure. Polarization measurements are shown in Table XXVI.

d. Cr^{+2}/Cr^{+3} (1N HCl)

$CrCl_2$ solubility in HCl continued to pose problems in this phase of the program. A pound of $CrCl_2$ was purchased from ROC/RIC Chemicals. Their catalogue lists $CrCl_2$ as very soluble in H_2O. Therefore, we attempted to dissolve this material in both H_2O and HCl (in various concentrations: 1M, 3M, 6M) using a glove box under N_2 atmosphere. Results

TABLE XXIII $Cu(NH_3)_2^{+1}/Cu(NH_3)_4^{+2}$ - POLARIZATION MEASUREMENTS

CONCENTRATION - 1M $Cu(NH_3)_2^{+1}/Cu(NH_3)_4^{+2}$ (1M NaCl + 0.01M NaOH)

ELECTRODE - Au screen - frontal structure

FLOW RATE - 300 cc/min.

MEMBRANE - Nafion-120

Total Conc	Polarization (mV)			
1M	1/4 (Reduced/Oxidized)			
Current Den.	27°C		50°C	
mA/cm^2	Anodic	Cathodic	Anodic	Cathodic
1	5	5	2	3
3	15	16	7	8
6	32	30	14	11
12	65	62	30	23
25	165	86	45	40
50	357	129	143	37*
100	674	854	285	56*
200				
400				

Total Conc	Polarization (mV)			
1M	5/1 (Reduced/Oxidized)			
Current Den.	27°C		50°C	
mA/cm^2	Anodic	Cathodic	Anodic	Cathodic
1	7	5	4	1
3	24	15	8	4
6	41	33	15	10
12	76	71	24	22
25	109	207	45	57
50	139	478	51	127
100	66*	1155	65	358
200	37*	1985	51*	691
400				

*iR correction large

TABLE XXIV $Cu(NH_3)_2^{+1}/Cu(NH_3)_4^{+2}$ - POLARIZATION MEASUREMENTS

CONCENTRATION - 1M $Cu(NH_3)_2^{+1}/Cu(NH_3)_4^{+2}$ (1M NaCl + 0.01M NaOH)

ELECTRODE - 5 mg/cm^2 Vulcan carbon (20% TFE) on gold grid-recessed structure

FLOW RATE - 300 cc/min.

MEMBRANE - Nafion-120

Total Conc	Polarization (mV)			
1M	1/4 (Reduced/Oxidized)			
Current Den.	27°C		50°C	
mA/cm^2	Anodic	Cathodic	Anodic	Cathodic
1	19	16	6	6
3	58	50	19	13
6	124	98	46	27
12	314	183	105	44
25	1353	333	1103	81
50	1803	349	1231	62*
100			1567	27*
200				
400				

Total Conc	Polarization (mV)			
1M	5/1 (Reduced/Oxidized)			
Current Den.	27°C		50°C	
mA/cm^2	Anodic	Cathodic	Anodic	Cathodic
1	33	11	4	3
3	99	34	12	7
6	184	78	20	17
12	345	171	38	37
25	537	494	63	96
50	715	1166	125	217
100	445*	2666	155	550
200	505*		179	
400				

*iR correction large

TABLE XXV $Cu(NH_3)_2^{+1}/Cu(NH_3)_4^{+2}$ - POLARIZATION MEASUREMENTS

CONCENTRATION 1M $Cu(NH_3)_2^{+1}/Cu(NH_3)_4^{+2}$ (1M NaCl + 0.01M NaOH)

ELECTRODE - 4.5 mg/cm^2 Vulcan carbon (20% TFE), activated with 0.5 mg/cm^2 gold, on gold grid support - Frontal Structure

FLOW RATE - 300 cc/min

MEMBRANE - Nafion-120

Total Conc	Polarization (mV)			
1M	1/4 (Reduced/Oxidized)			
Current Den.	27°C		50°C	
mA/cm^2	Anodic	Cathodic	Anodic	Cathodic
1	20	14	4	3
3	58	43	10	9
6	118	83	19	14
12	248	165	40	25
25	523	301	95	42
50	1037	456	210	55
100	1142	851	530	
200	1182	1371		
400				

Total Conc	Polarization (mV)			
1M	5/1 (Reduced/Oxidized)			
Current Den.	27°C		50°C	
mA/cm^2	Anodic	Cathodic	Anodic	Cathodic
1	12	8	1	2
3	33	18	1	4
6	74	71	2	9
12	153	128	3	15
25	445	336	11	76
50	748	605	41	122
100	877	1434	400	293
200				
400				

TABLE XXVI $Cu(NH_3)_2^{+1}/Cu(NH_3)_4^{+2}$ - POLARIZATION MEASUREMENTS

CONCENTRATION 1M $Cu(NH_3)_2^{+1}/Cu(NH_3)_4^{+2}$ - (1M NaCl + 0.01M NaOH)

ELECTRODE - 4.5 mg/cm^2 Vulcan carbon (20% TFE), activated with

FLOW RATE - 0.5 mg/cm^2 gold on gold grid support - recessed structur
300cc/min.

MEMBRANE - Nafion-120

Total Conc	Polarization (mV)			
1M	1/4 (Reduced/Oxidized)			
Current Den.	27°C		50°C	
mA/cm^2	Anodic	Cathodic	Anodic	Cathodic
1	47	19	10	10
3	147	59	34	28
6	380	113	70	63
12	1143	215	162	122
25	1849	360	1116	224
50	2489	541	1450	410
100			1885	638
200				
400				

Total Conc	Polarization (mV)			
1M	5/1 (Reduced/Oxidized)			
Current Den.	27°C		50°C	
mA/cm^2	Anodic	Cathodic	Anodic	Cathodic
1	23	9	5	3
3	66	28	11	7
6	120	63	18	17
12	229	147	34	33
25	256	433	50	106
50	323	1010	75	220
100		1690	56*	602
200				
400				

*iR correction large

with H_2O and HCl were the same. A small amount did seem to dissolve forming a blue-green solution, but gassing started immediately, and the mixtures became very hot, especially those with acid. When the reaction settled down, there was a large amount of sludge on the bottom of the container and some chromous chloride in solution.

A number of manufacturers of $CrCl_2$ were contacted about this problem of insolubility without much success. It has been suggested that the solubility problem might be the result of the method of preparation of the $CrCl_2$ used by the manufacturer, i.e. if the reduced form of the chloride was made by H_2-reduction of the hydrated oxidized form, then insoluble oxychlorides could be formed very easily; if an anhydrous oxidized form was used instead, the pure (soluble) chromous chloride would result. Therefore, the problem may have been that there was some oxychloride mixed with the chromous chloride in all of our samples. This seemed plausible in view of the fact that the chemicals we had purchased were all very green-grey, and $CrCl_2$ is reported to be white in the Handbook of Physics and Chemistry. Unfortunately, chemical manufacturers were reluctant to reveal the method by which they prepared their $CrCl_2$ so that we were unable to locate an appropriate source of this material.

Because of these solubility problems, we attempted to form the Cr^{+2} electrolytically in solution from Cr^{+3} in two redox ratios: a 1M 1:4 and a 1M 6.25:1 solution. The 1M 1:4 solution preparation was successful, and this solution was tested. However, we were unable to complete preparation of the 1M 6.25:1 solution. The final composition that we obtained was $\sim$ 3:2 ratio and attempts to reduce it further were not practical. The time for Cr^{+3} reduction to Cr^{+2} was excessively long, and

the efficiency of conversion had dropped to ∿ 10%. Therefore, this solution was used only as the counter electrode solution in testing the 1M 1:4 preparation.

The membrane used for the Cr^{+2}/Cr^{+3} couple was 103-QZL-183. As mentioned above problems had been occurring with this particular membrane. After operation at 50°C, the membrane generally developed cracks. On the recommendation of Ionics, we pretreated the membrane in 1NHCl at 50°C - 60°C for one hour before assembling the cell. This procedure alleviated the cracking problem in subsequent operation of the cell.

i. Au Screen - Frontal Structure. This electrode was a gold expanded mesh in a frontal structure. During the course of these and the following measurements a reddish-brown coating was observed to form on the walls of the reservoir and the surface of the electrode, possibly indicating the precipitation of $CrCl_2$ during operation.

Polarization measurements are shown in Table XXVII.

ii. Porous Carbon - Recessed Structure. This electrode consisted of 5 mg/cm^2 Vulcan carbon (20% Teflon as binder) on a gold plated tantalum screen support in a recessed structure. Polarization measurements are shown in Table XXVIII.

iii. Au-Activated Carbon - Frontal Structure. This electrode consisted of Vulcan carbon (20% Teflon) activated with 0.5 mg Au/cm^2 on a gold plated tantalum screen support. The structure was frontal. Polarization measurements are shown in Table XXIX.

iv. Au-Activated Carbon - Recessed Structure. This electrode consisted of 4.5 mg/cm^2 Vulcan carbon (20% Teflon binder)

activated with 0.5 mg/cm^2 Au on gold plated tantalum screen support. The structure was recessed. Polarization measurements are shown in Table XXX.

TABLE XXVII Cr^{+2}/Cr^{+3} - POLARIZATION MEASUREMENTS

CONCENTRATION - 1M $CrCl_2/CrCl_3$ (1M HCl)

ELECTRODE - Au Screen - Frontal Structure

FLOW RATE - 300 cc/min.

MEMBRANE - 103-QZL-183

Total Conc	Polarization (mV)			
1M	1/4 (Reduced/Oxidized)			
Current Den.	27°C		50°C	
mA/cm^2	Anodic	Cathodic	Anodic	Cathodic
1	126	141	27	38
3	146	207	53	84
6	161	1020	137	123
12	181	1074	161	743
25	190	1094	178	1025
50	190*	1127	182	1045
100		1210		
200				
400				

*iR correction large

TABLE XXVIII Cr^{+2}/Cr^{+3} - POLARIZATION MEASUREMENTS

CONCENTRATION - 1M $CrCl_2/CrCl_3$ (1M HCl)

ELECTRODE - 5 mg/cm^2 Vulcan Carbon (20% TFE) on gold plated tantalum screen - recessed structure

FLOW RATE - 300 cc/min.

MEMBRANE - 103-QZL-183

Total Conc	Polarization (mV)			
1M	1/4 (Reduced/Oxidized)			
Current Den.	27°C		50°C	
mA/cm^2	Anodic	Cathodic	Anodic	Cathodic
1	148	78	28	167
3	208	141	77	204
6	243	516	105	479
12	347	1226	162	746
25	559	1320	254	1374
50	657	1428	606	1431
100	1313	1557	723	
200	---	-		
400				

TABLE XXIX Cr^{+2}/Cr^{+3} - POLARIZATION MEASUREMENTS

CONCENTRATION - 1M $CrCl_2/CrCl_3$ (1M HCl)

ELECTRODE - 4.5 mg/cm^2 Vulcan carbon (20% TFE), activated with 0.5 mg Au on gold plated tantalum screen, frontal structure

FLOW RATE - 300 cc/min.

MEMBRANE - 103-QZL-183

Total Conc	Polarization (mV)			
1M	1/4 (Reduced/Oxidized)			
Current Den.	27°C		50°C	
mA/cm^2	Anodic	Cathodic	Anodic	Cathodic
1	58	93	35	6
3	88	196	46	174
6	102	348	132	236
12	115	944	324	671
25	134	1167	540	1082
50	469	1290	603	1129
100	539	------	672	1217
200				
400				

TABLE XXX Cr^{+2}/Cr^{+3} POLARIZATION MEASUREMENTS

CONCENTRATION - 1M $CrCl_2/CrCl_3$ (1M HCl)

ELECTRODE - 4.5 mg/cm^2 Vulcan carbon (20% TFE), activated with 0.5 mg Au, on gold plated tantalum screen-recessed structure

FLOW RATE - 300 cc/min.

MEMBRANE - 103-QZL-183

Total Conc	Polarization (mV)			
1M	1/4 (Reduced/Oxidized)			
Current Den.	27°C		50°C	
mA/cm^2	Anodic	Cathodic	Anodic	Cathodic
1	111	95	375	162
3	144	152	444	1174
6	175	579	502	1443
12	296	1008	540	2010
25	359	1163	652	2039
50	505	1211	867	2127
100	577	1340	928	
200				
400				

TABLE XXXI. OPEN CIRCUIT POTENTIALS VS. SATURATED CALOMEL ELECTRODE

Redox Couple	OCV vs. SCE (Volts)							
	86% charged				80% discharged			
	27°C		50°C		27°C		50°C	
Fe^{+2}/Fe^{+3}	1M	3M	1M	3M	1M	3M	1M	3M
(1M HCl)	0.47	0.48	0.49	0.49	0.43	0.42	0.45	0.42
	86% charged				80% discharged			
	27°C				27°C			
Br^-/Br_3^-	3N	9N			3N	9N		
(NaBr)	0.82	0.79			0.77	0.75		
	83% charged				80% discharged			
	27°C		50°C		27°C		50°C	
$Cu(NH_3)_2^{+1}/Cu(NH_3)_4^{+2}$	1M		1M		1M		1M	
(1M NaCl + 0.01 NaOH)	-0.39		-0.35		-0.30		-0.28	
					80% discharged			
					27°C		50°C	
Cr^{+2}/Cr^{+3}					1M		1M	
(1M HCl)					-0.69		-0.66	

C. DISCUSSION OF THE RESULTS OF TASK II

In order to compare the effect of different electrode structures and materials on the performance of redox flow reactors the data presented in Tables XV through XXX have been rearranged as shown in Tables XXXII through XLV to show the performance of all four electrodes for a particular redox couple, under fixed conditions of concentration and temperature. Because of the large number of variables studied, as called for by the Work Statement of this Contract, optimization of structures and operating conditions (flow rate, electrolyte gap, membrane, etc.) and considerations of flow reactor theory, have not been possible. Conclusions regarding electrode structure and materials apply only to the very specific structures and conditions used; conclusions regarding concentration and temperature are intended to show broad trends.

Comparison of the performance of the different electrode configurations for the Fe^{+2}/Fe^{+3} couple (Table XXXII to XXXV) shows that in general structure D, a "within the cavity"structure, based on graphite cloth (as used at NASA-Lewis) delivers the best performance of all the tested structures, in the current density range prior to a clear concentration limitation. Next in performance was structure B, followed by A (both recessed structures). Structure C, a frontal structure, was the least effective. It should be kept in mind, however, that in all cases iR drop has been eliminated; this means that, in addition to the iR drop of the membrane and any iR drop attributable to the counter electrode (which will be the same in the tests of the four structures), the electrolyte resistance intrinsic to a recessed structure has also been eliminated The contribution of this iR-drop can be changed by changing the size of the electrolyte gap. In Table XLVI, iR values are shown for the gap used in this

study, at a current density of 100 mA/cm^2. Also, it should be repeated that the poorer performance observed with the frontal structure applies only to the specific structure used here, a rather open meshed screen (80 mesh), and is not a general conclusion applicable to all frontal structures.

There are indications in the test data for the Fe^{+2}/Fe^{+3} couple that in cases of low reactant concentration (such as charging from charged state, Table XXXV) electrode structure D (graphite cloth) becomes diffusion limited at rather low current densities. In such cases, the other structures may have higher limiting currents. The relative merits of the different structures must also be evaluated in terms of the effect of flow rate and the impact of this flow rate on pumping requirements for each structure, especially when comparing the vastly different conditions of frontal and recessed structures on the one hand, and cavity filling structures (flow through porous structures) on the other hand. Such effects are best studied in a systematic manner using electrochemical reactor theory.

In the redox flow reactor experiments with the Br^-/Br_3^- couple (Tables XXXVI to XXXIX) the best short-term, iR-corrected, performance was obtained with electrode A, a thick porous carbon recessed structure, followed very closely in performance by electrode B, a thin graphite-paper, frontal structure. (Same comments regarding iR-correction for Fe^{+2}/Fe^{+3} apply here, see Table XLVI). In general, the short-term performance with the Br^-/Br_3^- couple is quite encouraging. Selection of electrode materials for the long-term, practical tests must consider corrosion effects.

The $Cu(NH_3)_2^{+1}/Cu(NH_3)_4^{+2}$ couple showed moderate performance under conditions of high concentration of reactant (Tables XL and XLII). The performance deteriorated markedly under the studied conditions, in all cases of depleted

reactant (Table XLI to XLIII). In the latter cases increasing temperature tended to increase the limiting current substantially. The best performance was obtained with electrode A, followed by electrode C (both are frontal structures activated with gold).

The experiments with the Cr^{+2}/Cr^{+3} couple showed very high polarizations in all cases, even at current densities lower than 3 mA/cm^2. Differences between structures are not significant under these conditions.

C-2

TABLE XXXII. COMPARISON OF ELECTRODE CONFIGURATION PERFORMANCE FOR THE Fe^{+2}/Fe^{+3} COUPLE (DISCHARGING IN THE CHARGED STATE)

Red/Ox ratio = 1/6.25; Cathodic Performance

Total Conc. 1M Temp. 27°C				
Current Density (mA/cm^2)	Polarization (mV)			
	A*	B	C	D
1	3	1	2	-
3	4	3	8	1
6	9	5	16	-
12	18	11	31	3
25	40	24	63	11
50	83	43	122	26
100	193	101	234	81
200	525	323	436	116
400	925	864	812	1396

Total Conc. 3M Temp. 27°C				
Current Density (mA/cm^2)	Polarization (mV)			
	A	B	C	D
1	3	2	4	1
3	11	4	13	4
6	24	6	25	7
12	49	14	52	17
25	104	24	109	48
50	192	34	217	99
100	358	148	435	232
200	748	587	812	407
400		897		497

Total Conc. 1M Temp. 50°C				
Current Density (mA/cm^2)	Polarization (mV)			
	A	B	C	D
1	1	1	-	-
3	5	3	1	2
6	6	4	6	4
12	12	10	16	-
25	26	20	33	13
50	37	38	65	34
100	117	80	131	87
200	332	168	253	109
400	939	343	497	249

Total Conc. 3M Temp. 50°C				
Current Density (mA/cm^2)	Polarization (mV)			
	A	B	C	D
1	3	3	-	1
3	6	5	4	3
6	12	7	11	4
12	26	15	25	10
25	57	29	50	28
50	119	48	106	64
100	295	186	226	156
200	592	303	426	295
400	602	683	898	528

* Configurations: A - 5 mg/cm^2 Vulcan Carbon (20% TFE) on gold plated tantalum screen - recessed structure

B - 0.5 mg Pt/cm^2 on 4.5 mg Vulcan Carbon/cm^2 (20% TFE) on gold screen - recessed structure

C - Pt screen - frontal st ucture

D - Graphite Cloth Electrode "Within the Cavity" structure

TABLE XXXIII. COMPARISON OF ELECTRODE CONFIGURATION PERFORMANCE FOR THE Fe^{+2}/Fe^{+3} COUPLE (DISCHARGING IN DISCHARGED STATE)

Red/Ox ratio = 4/1; Cathodic Performance

Total Conc. 1M Temp. 27°C				
Current Density (mA/cm^2)	Polarization (mV)			
	A*	B	C	D
1	1	3	2	-
3	2	9	5	2
6	6	17	11	5
12	13	36	23	11
25	31	75	49	24
50	67	132	97	47
100	149	216	193	121
200	557	764	441	148
400	1597	894	1444	1430

Total Conc. 3M Temp. 27°C				
Current Density (mA/cm^2)	Polarization (mV)			
	A	B	C	D
1	6	2	3	1
3	13	6	8	3
6	20	9	17	6
12	37	20	34	11
25	73	40	70	26
50	151	71	135	49
100	671	213	274	126
200	1816	1045	536	231
400		1525		1431

Total Conc. 1M Temp. 50°C				
Current Density (mA/cm^2)	Polarization (mV)			
	A	B	C	D
1	1	1	-	-
3	2	3	2	1
6	4	7	5	2
12	10	13	12	6
25	21	30	27	12
50	42	61	54	22
100	84	92	113	74
200	255	119	222	123
400	1259	565	476	1290

Total Conc. 3M Temp. 50°C				
Current Density (mA/cm^2)	Polarization (mV)			
	A	B	C	D
1	-	-	2	-
3	-	1	5	-
6	1	2	10	2
12	4	6	19	4
25	9	15	38	7
50	20	33	73	8
100	75	41	153	56
200	182	185	303	103
400		608	635	1654

*-Configurations: A - 5 mg/cm^2 Vulcan Carbon (20% TFE) on gold plated tantalum screen - recessed structure

B - 0.5 mg Pt/cm^2 on 4.5 mg Vulcan Carbon/cm^2 (20% TFE) on gold screen - recessed structure

C - Pt screen - frontal structure

D - Graphite Cloth Electrode "Within the Cavity" structure

TABLE XXXIV. COMPARISON OF ELECTRODE CONFIGURATION PERFORMANCE FOR THE Fe^{+2}/Fe^{+3} COUPLE (CHARGING IN THE DISCHARGED STATE)

Red/Ox ratio = 4/1; Anodic Performance

Total Conc. 1M Temp. 27°C				
Current Density (mA/cm^2)	Polarization (mV)			
	A*	B	C	D
1	-	6	2	-
3	2	19	7	1
6	3	38	13	2
12	6	76	25	4
25	12	152	54	8
50	24	279	101	13
100	59	366	205	40
200	188	448	403	268
400	993	546	758	1290

Total Conc. 3M Temp. 27°C				
Current Density (mA/cm^2)	Polarization (mV)			
	A	B	C	D
1	8	1	2	-
3	16	2	8	1
6	40	6	16	5
12	90	8	35	10
25	187	18	74	25
50	357	38	150	50
100	686	99	302	172
200	1075	223	591	309
400	1495	606		529

Total Conc. 1M Temp. 50°C				
Current Density (mA/cm^2)	Polarization (mV)			
	A	B	C	D
1	1	2	-	1
3	2	6	2	2
6	3	13	5	3
12	6	25	14	6
25	15	56	30	10
50	30	156	59	18
100	66	265	122	48
200	146	295	245	177
400	761	385	494	560

Total Conc. 3M Temp. 50°C				
Current Density (mA/cm^2)	Polarization (mV)			
	A	B	C	D
1	1	-	1	-
3	-	2	3	1
6	2	2	7	-
12	4	2	15	3
25	7	6	34	7
50	13	12	73	10
100	30	101	150	38
200	58	-	308	92
400	162	-	628	357

* Configurations: A - 5 mg/cm^2 Vulcan Carbon (20% TFE) on gold plated tantalum screen - recessed structure

B - 0.5 mg Pt/cm^2 on 4.5 mg Vulcan Carbon/cm^2 (20% TFE) on gold screen - recessed structure

C - Pt screen - frontal structure

D - Graphite Cloth Electrode "Within the Cavity" structure

TABLE XXXV. COMPARISON OF ELECTRODE CONFIGURATION PERFORMANCE FOR THE Fe^{+2}/Fe^{+3} COUPLE (CHARGING IN CHARGED STATE)

Red/Ox ratio = 1/6.25; Anodic Performance

Total Conc. 1M Temp. 27°C				
Current Density (mA/cm^2)	Polarization (mV)			
	A*	B	C	D
1	1	1	2	6
3	4	-	6	6
6	7	2	14	7
12	16	3	28	7
25	35	10	60	12
50	74	24	126	18
100	173	167	276	448
200	585	676	816	908
400		816	1435	3018

Total Conc. 3M Temp. 27°C				
Current Density (mA/cm^2)	Polarization (mV)			
	A	B	C	D
1	4	1	4	1
3	10	-	12	3
6	20	2	25	5
12	41	5	50	11
25	80	14	106	16
50	173	27	217	-
100	445	168	481	55
200	972	353	1239	603
400		553		623

Total Conc. 1M Temp. 50°C				
Current Density (mA/cm^2)	Polarization (mV)			
	A	B	C	D
1	2	1	-	-
3	8	2	1	1
6	17	4	5	3
12	36	8	12	5
25	77	17	29	14
50	152	34	62	29
100	207	105	132	232
200	421	200	272	878
400	941	785	683	3438

Total Conc. 3M Temp. 50°C				
Current Density (mA/cm^2)	Polarization (mV)			
	A	B	C	D
1	3	1	-	1
3	6	3	3	3
6	12	5	9	5
12	23	8	23	9
25	42	18	51	13
50	96	35	106	20
100	120	92	226	80
200	393	194	495	278
400		474	1215	

* Configurations:
A - 5 mg/cm^2 Vulcan Carbon (20% TFE) on gold plated tantalum screen - recessed structure

B - 0.5 mg Pt/cm^2 on 4.5 mg Vulcan Carbon/cm^2 (20% TFE) on gold screen - recessed structure

C - Pt screen - frontal structure

D - Graphite Cloth Electrode "Within the Cavity" structure

TABLE XXXVI. COMPARISON OF ELECTRODE CONFIGURATION PERFORMANCE FOR THE Br^-/Br_3^- COUPLE (DISCHARGING IN CHARGED STATE)

Red/Ox ratio = 1/6.25; Cathodic Performance

Total Conc. 3N Temp. 27°C				
Current Density (mA/cm^2)	Polarization (mV)			
	A*	B	C	D
1	-	1	1	4
3	1	3	2	9
6	2	4	4	11
12	3	9	7	19
25	7	17	16	33
50	13	36	43	61
100	48	92	95	136
200	68		619	204
400				

Total Conc. 9N Temp. 27°C				
Current Density (mA/cm^2)	Polarization (mV)			
	A	B	C	D
1	1	2	1	3
3	2	3	3	4
6	2	5	5	6
12	6	10	6	12
25	11	21	21	25
50	25	37	25	43
100	41	81	27	70
200	70	117	111	160
400				

*Configurations: A - Porous Carbon - recessed structure

B - Teflonated Graphite Paper (4.5 mg TFE/cm^2) - frontal structure

C - Platinized Ti Sheet - recessed structure

D - 4.5 mg RuO_2 on Ti Screen - frontal structure

TABLE XXXVII.- COMPARISON OF ELECTRODE CONFIGURATION PERFORMANCE FOR THE Br^-/Br_3^- COUPLE (DISCHARGING IN DISCHARGED STATE)

Red/Ox ratio = 4/1; Cathodic performance

Total Conc. 3N Temp. 27°C				
Current Density (mA/cm^2)	Polarization (mV)			
	A*	B	C	D
1	-	5	5	1
3	2	6	6	4
6	5	8	10	5
12	10	13	18	12
25	20	25	35	27
50	39	43	58	54
100	77	92	227	123
200	151	147	332	185
400				

Total Conc. 9N Temp. 27°C				
Current Density (mA/cm^2)	Polarization (mV)			
	A	B	C	D
1	1	4	4	2
3	3	10	17	6
6	6	17	18	12
12	11	33	33	25
25	23	58	61	47
50	33	91	100	85
100	38	97	111	94
200		181	150	168
400				

*Configurations: A - Porous Carbon - recessed structure

B - Teflonated Graphite Paper (4.5 mg TFE/cm^2) - frontal structure

C - Platinized Ti Sheet - recessed structure

D - 4.5 mg RuO_2 on Ti Screen - frontal structure

TABLE XXXVIII. COMPARISON OF ELECTRODE CONFIGURATION PERFORMANCE FOR THE Br^-/Br_3^- COUPLE (CHARGING IN DISCHARGED STATE)

Red/Ox ratio = 4/1; Anodic performance

Total Conc. 3N Temp. 27°C				
Current Density (mA/cm^2)	Polarization (mV)			
	A*	B	C	D
1	1	1	5	
3	3	2	14	3
6	8	4	26	5
12	13	10	48	11
25	23	20	85	22
50	37	35	144	42
100	70	63		83
200	83	83		111
400				

Total Conc. 9N Temp. 27°C				
Current Density (mA/cm^2)	Polarization (mV)			
	A	B	C	D
1	1	2	4	2
3	3	3	18	4
6	4	4	21	6
12	5	7	41	13
25	20	23	85	29
50	45	52	155	72
100	165	129	377	208
200	304		604	356
400				

*Configurations: A - Porous Carbon - recessed structure

B - Teflonated Graphite Paper (4.5 mg TFE/cm^2) - frontal structure

C - Platinized Ti Sheet - recessed structure

D - 4.5 mg RuO_2 on Ti Screen - frontal structure

TABLE XXXIX. COMPARISON OF ELECTRODE CONFIGURATION PERFORMANCE FOR THE Br^-/Br_3^- COUPLE (CHARGING IN CHARGED STATE)

Red/Ox ratio = 1/6.25; Anodic performance

Total Conc. 3N Temp. 27°C				
Current Density (mA/cm^2)	Polarization (mV)			
	A*	B	C	D
1	-	2	6	1
3	1	5	16	4
6	2	8	31	8
12	5	13	52	18
25	8	28	92	31
50	16	49	142	57
100	24	117		100
200				116
400				

Total Conc. 9N Temp. 27°C				
Current Density (mA/cm^2)	Polarization (mV)			
	A	B	C	D
1	1	2	2	1
3	- 2	3	5	3
6	3	5	9	7
12	6	7	18	12
25	11	16	32	24
50	24	28	51	48
100	36	38		74
200	75	59		156
400				

*Configurations: A - Porous Carbon-- recessed structure

B - Teflonated Graphite Paper (4.5 mg TFE/cm^2) - frontal structure

C - Platinized Ti Sheet - recessed structure

D - 4.5 mg RuO_2 on Ti Screen - frontal structure

TABLE XL. COMPARISON OF ELECTRODE CONFIGURATION PERFORMANCE FOR THE $Cu(NH_3)_2^{+1}/Cu(NH_3)_4^{+2}$ COUPLE (DISCHARGING IN CHARGED STATE)

Red/Ox ratio = 5/1; Anodic Performance

Total Conc. 1M Temp. 27°C				
Current Density (mA/cm^2)	Polarization (mV)			
	A*	B	C	D
1	7	33	12	23
3	24	99	33	66
6	41	184	74	120
12	76	345	153	229
25	109	537	445	256
50	139	115†	748	323
100	66†	445†	877	
200	37†	505†		
400				

Total Conc. 1M Temp. 50°C				
Current Density (mA/cm^2)	Polarization (mV)			
	A	B	C	D
1	4	4	1	5
3	8	12	1	11
6	15	20	2	18
12	24	38	3	34
25	45	63	11	50
50	51	125	41	78
100	65	155	400	56†
200	51†	179		
400				

†iR correction large

*Configurations - A - Au screen - frontal structure

B - 5 mg/cm^2 Vulcan carbon (20% TFE) on gold grid - recessed structure

C - 4.5 mg/cm^2 Vulcan carbon (20% TFE), activated with 0.5 mg/cm^2 gold, on gold grid support - frontal structure

D - 4.5 mg/cm^2 Vulcan carbon (20% TFE), activated with 0.5 mg/cm^2 gold on gold grid support - recessed structure

TABLE XLI. COMPARISON OF ELECTRODE CONFIGURATION PERFORMANCE FOR THE $Cu(NH_3)_2^{+1}/Cu(NH_3)_4^{+2}$ COUPLE (DISCHARGING IN DISCHARGED STATE)

Red/Ox ratio = 1/4; Anodic Performance

Total Conc. 1M			Temp. 27°C	
Current Density (mA/cm^2)	Polarization (mV)			
	A*	B	C	D
1	5	19	20	47
3	15	58	58	147
6	32	124	118	380
12	65	314	248	1143
25	165	1353	523	1849
50	357	1803	1037	2489
100	674		1142	
200			1182	
400				

Total Conc.			Temp.	
Current Density (mA/cm^2)	Polarization (mV)			
	A	B	C	D
1	2	6	4	10
3	7	19	10	34
6	14	46	19	70
12	30	105	40	162
25	45	1103	95	1116
50	143	1231	210	1450
100	285	1567	530	1885
200				
400				

*Configurations - A - Au screen - frontal structure

B - 5 mg/cm^2 Vulcan carbon (20% TFE) on gold grid - recessed structure

C - 4.5 mg/cm^2 Vulcan carbon (20% TFE), activated with 0.5 mg/cm^2 gold, on gold grid support - frontal structure

D - 4.5 mg/cm^2 Vulcan carbon (20% TFE), activated with 0.5 mg/cm^2 gold on gold grid support - recessed structure

TABLE XLII. COMPARISON OF ELECTRODE CONFIGURATION PERFORMANCE FOR THE $Cu(NH_3)_2^{+1}/Cu(NH_3)_4^{+2}$ COUPLE (CHARGING IN DISCHARGED STATE)

Red/Ox ratio = 1/4; Cathodic performance

Total Conc. 1M	Temp. 27°C			
Current Density (mA/cm^2)	Polarization (mV)			
	A*	B	C	D
1	5	16	14	19
3	16	50	43	59
6	30	98	83	113
12	62	183	165	215
25	86	333	301	360
50	129	349	456	541
100	854		851	
200			1371	
400				

Total Conc. 1M	Temp. 50°C			
Current Density (mA/cm^2)	Polarization (mV)			
	A	B	C	D
1	3	6	3	10
3	8	13	9	28
6	11	27	14	63
12	23	44	25	122
25	40	81	42	224
50	37†	62†	55	410
100	56	27†		638
200				
400				

†iR correction large

*Configurations - A - Au screen - frontal structure

B - 5 mg/cm^2 Vulcan carbon (20% TFE) on gold grid - recessed structure

C - 4.5 mg/cm^2 Vulcan carbon (20% TFE), activated with 0.5 mg/cm^2 gold, on gold grid support - frontal structure

D - 4.5 mg/cm^2 Vulcan carbon (20% TFE), activated with 0.5 mg/cm^2 gold on gold grid support - recessed structure

TABLE XLIII. COMPARISON OF ELECTRODE CONFIGURATION PERFORMANCE FOR THE $Cu(NH_3)_2^{+1}/Cu(NH_3)_4^{+2}$ COUPLE (CHARGING IN CHARGED STATE)

Red/Ox ratio = 5/1; Cathodic Performance

Total Conc. 1M Temp. 27°C				
Current Density (mA/cm^2)	Polarization (mV)			
	A*	B	C	D
1	5	11	8	9
3	15	34	18	28
6	33	78	71	63
12	71	171	128	147
25	207	494	336	433
50	478	1166	605	1010
100	1155	2666	1434	1690
200	1985			
400				

Total Conc. 1M Temp. 50°C				
Current Density (mA/cm^2)	Polarization (mV)			
	A	B	C	D
1	1	3	2	3
3	4	7	4	7
6	10	17	9	17
12	22	37	15	33
25	57	96	76	106
50	127	217	122	220
100	358	550	293	602
200	691			
400				

*Configurations - A - Au screen - frontal structure

B - 5 mg/cm^2 Vulcan carbon (20% TFE) on gold grid - recessed structure

C - 4.5 mg/cm^2 Vulcan carbon (20% TFE), activated with 0.5 mg/cm^2 gold, on gold grid support - frontal structure

D - 4.5 mg/cm^2 Vulcan carbon (20% TFE), activated with 0.5 mg/cm^2 gold on gold grid support - recessed structure

TABLE XLIV. COMPARISON OF ELECTRODE CONFIGURATION PERFORMANCE FOR THE Cr^{+2}/Cr^{+3} COUPLE (DISCHARGING IN DISCHARGED STATE)

Red/Ox ratio = 1/4; Anodic performance

Total Conc. 1M Temp. 27°C				
Current Density (mA/cm^2)	Polarization (mV)			
	A*	B	C	D
1	126	148	58	111
3	146	208	88	144
6	161	243	102	175
12	181	347	115	296
25	190	559	134	359
50	190	657	469	505
100		1313	539	577
200				
400				

Total Conc. 1M Temp. 50°C				
Current Density (mA/cm^2)	Polarization (mV)			
	A	B	C	D
1	27	28	35	375
3	53	77	46	444
6	137	105	132	502
12	161	162	324	540
25	178	254	540	652
50	182	606	603	867
100		723	672	928
200				
400				

*Configurations: A - Au Screen - Frontal Structure

B - 5 mg/cm^2 Vulcan Carbon (20% TFE) on gold plated tantalum screen - recessed structure

C - 4.5 mg/cm^2 Vulcan carbon (20% TFE), activated with 0.5 mg Au on gold plated tantalum screen, frontal structure

D - 4.5 mg/cm^2 Vulcan carbon (20% TFE), activated with 0.5 mg Au, on gold plated tantalum screen - recessed structure

TABLE XLV. COMPARISON OF ELECTRODE CONFIGURATION PERFORMANCE FOR THE Cr^{+2}/Cr^{+3} COUPLE (CHARGING IN DISCHARGED STATE)

Red/Ox ratio = 1/4; Cathodic performance

Total Conc. 1M Temp. 27°C				
Current Density (mA/cm^2)	Polarization (mV)			
	A*	B	C	D
1	141	78	93	95
3	207	141	196	152
6	1020	516	348	579
12	1074	1226	944	1008
25	1094	1320	1167	1163
50	1127	1420	1290	1211
100	1210	1557		1340
200				
400				

Total Conc. 1M Temp. 50°C				
Current Density (mA/cm^2)	Polarization (mV)			
	A	B	C	D
1	38	167	6	162
3	84	204	174	1174
6	123	479	236	1443
12	743	746	671	2010
25	1025	1374	1082	2039
50	1045	1431	1129	2127
100			1217	
200				
400				

*Configurations: A - Au Screen - Frontal Structure

B - 5 mg/cm^2 Vulcan Carbon (20% TFE) on gold plated tantalum screen - recessed structure

C - 4.5 mg/cm^2 Vulcan carbon (20% TFE), activated with 0.5 mg Au on gold plated tantalum screen, frontal structure

D - 4.5 mg/cm^2 Vulcan carbon (20% TFE), activated with 0.5 mg Au, on gold plated tantalum screen - recessed structure

TABLE XLVI.

EXAMPLES OF iR CONTRIBUTION OF ELECTROLYTE

GAP IN RECESSED ELECTRODE STRUCTURES

	Red/Ox Ratio	Total Conc. (M)	Temp. (°C)	~ iR @ 100mA/cm^2 (mV)
A. Fe^{+1}/Fe^{+2}	1/6.25	1	27	85
			50	65
		3	27	210
			50	140
	4/1	1	27	75
			50	60
		3	27	135
			50	95
B. Br^-/Br_3^-	1/6.25	3N	27	230
		9N	27	105
	4/1	3N	27	150
		9N	27	85
C. $Cu(NH_3)_2^{+1}/Cu(NH_3)_4^{+2}$	5/1	1M	27	45
			50	25
	1/4	1M	27	230
			50	140
D. Cr^{+2}/Cr^{+3}	1/4	1M	27	115
			50	85

III. REFERENCES

1. A. Seidell and W.F. Linke, Solubilities of Inorganic and Metal Organic Compounds, Volume 1, p. 927, American Chemical Society, Washington, D.C. (1958).

2. ibid 443.

3. Handbook of Chemistry and Physics, 54th Edition, Ed. R.C. Weast, CRC Press, 1973.

4. J.E.B. Randles and K.W. Somerton, "Kinetics of Rapid Electrode Reactions," Trans. Faraday Soc., 48 p. 937 (1952).

5. D.N. Hume and I.M. Kolthoff, "The Oxidation-Potential of Chromocyanide-Chromicyanide Couples," J. Am. Chem. Soc., 65 p. 897 (1943).

6. K.J.Vetter, Electrochemische Kinetik, Springer-Verlag, Berlin, 1961 (German).

7. W.H. Tiedeman, J. Newman and D.N. Bennion, "The Error in Measurements of Electrode Kinetics Caused by Nonuniform Ohmic-Potential Drop to a Disk Electrode," J. Electrochem. Soc., Feb. 1973, 120(2) p. 256-258.

8. H. Lerner and L.G. Austin, "The Kinetics of the Stannous/Stannic Redox Reaction at Carbon Electrodes." J. Electrochem. Soc., 112(6) p. 636 (1965).

9. W. O'Grady, C. Iwakura, J. Huang, and Ernest Yeager, "Ruthenium Oxide Catalysts for the Oxygen Electrode," from Electrocatalysis p. 286, Ed. M. W. Breiter, Electrochemical Society, 1974.

10. J. Giner, J.M. Parry and S.M. Smith, "Preparation of Platinum Black for Anodic Hydrocarbon Oxidation," Advances in Chemistry Series, No. 90, Fuel Cell Systems II, p. 151, American Chemical Society, 1969.

11. D.J. Pickett and B.R. Stanmore, J. Applied Electrochem., 2 p. 151 (1972).

APPENDIX I

Stoichiometry of the Bromine Redox Couple

In calculating the number of moles of Br_2 (M_{Br_2}) and of NaBr (M_{NaBr}) to simulate a particular state of the Br_3^-/Br^- redox couple, two parameters are fixed: the total number of atom weights of Bromine in the system, $(Br)_T$, and the theoretical degree of discharge, θ. The theoretical degree of discharge can be defined by writing equation:

$$\frac{1-\theta}{2} Br_3^- + \theta e^- \rightarrow \frac{3}{2}\theta\, Br^- \qquad (1)$$

When the system is totally charged, $\theta = 0$; when the system is totally discharged, $\theta = 1$. The condition of totally charged system and the manner of writing equation (1) imply that no Br_2 is allowed to form. This is equivalent to saying that any Br_2 formed will react with excess Br^- to form Br_3^- and that an additional reaction of the form:

$$2Br_3^- + 2e^- \rightarrow 3Br_2 \qquad (2)$$

is not allowed. Under these conditions, the vapor pressure of bromine will be lowest.

According to equation (1) the total bromine per Faraday of charge is given by:

$$(Br)_T = 3\,\frac{1-\theta}{2} + \frac{3}{2}\theta = \frac{3}{2} \qquad (3)$$

The number of moles of bromine for a given degree of discharge and total bromine:

$$M_{Br_3^-} = M_{Br_2} = \frac{1-\theta}{3}(Br)_T \qquad (4)$$

$$Br_2 \text{ (atom equiv.)} = \frac{2}{3}(1-\theta)(Br_T)$$

(i.e. only 66.66% of total bromine atoms can be charged according to equation (1).)

Similarly, the number of moles of <u>free</u> Br^- is given by:

$$M_{Br^-} = \theta\ (Br)_T \tag{5}$$

The ratio of reduced to oxidized species defined as $\frac{Red}{Ox} \equiv \frac{M_{Br^-}}{M_{Br_3^-}}$ is related to the degree of discharge by:

$$\frac{Red}{Ox} = \frac{3}{1 - \theta} - 3 \tag{6}$$

The number of moles of Br_2 and of NaBr required to prepare a solution with a fixed total number of bromine atoms, and simulating a degree of discharge θ is:

$$M_{Br_2} = (Br)_T \frac{1 - \theta}{3} \tag{7a}$$

$$M_{NaBr} = (Br)_T \frac{1 + 2\theta}{3} \tag{7b}$$

The molar ratio of sodium bromide to bromine needed to simulate a certain state of discharge is given by:

$$\frac{M_{NaBr}}{M_{Br_2}} = \frac{3}{1 - \theta} - 2 \tag{8}$$

The ratio of reduced to oxidized species is related to the molar ratio of sodium bromide to bromine used to prepare the solution by:

$$\frac{Red}{Ox} = \frac{M_{Br^-}}{M_{Br_3^-}} = \frac{M_{NaBr}}{M_{Br_2}} - 1 \tag{9}$$

Moles of Br_2 and NaBr necessary to prepare a solution with a fixed number of atom weights of Bromine $(Br)_T$ and with a given Red/Ox-ratio is obtained as follows:

From (7a) and (6):

$$M_{Br_2} = \frac{(Br)_T}{3 + \frac{Red}{Ox}} \tag{10a}$$

From (7b) and (6):

$$M_{NaBr} = (Br)_T \left(1 - \frac{2}{3 + \frac{Red}{Ox}}\right) \qquad (10b)$$

Instead of the molar ratio of reduced to oxidized species $\frac{Red}{Ox}$ as used here, one could use the ratio of equivalent weights $\left(\frac{Red}{Ox'}\right)$ (where $Ox' = 2\ Ox$). Such use involves substituting $\left(\frac{Red}{Ox}\right)$ by $2\left(\frac{Red}{Ox'}\right)$ in equations (6), (9), (10).

APPENDIX II

Concentration Dependence on Exchange Current

Under ideal conditions, the exchange current of a one-electron redox reaction is related to the concentrations of reduced and oxidized species by:

$$i_o = i_o^o (Red)^{\alpha} (Ox)^{\beta}$$

where α and β are transfer coefficients. If $\alpha = 1 - \beta = 0.5$, for instance, the exchange current of the 1:10 redox ratio, $i_{o(1:10)}$, will be equal to that of the 10:1 ratio, $i_{o(10:1)}$, and will be related to the exchange current for (1:1) ratio, $i_{o(1:1)}$, by:

$$i_{o(1:10)} = i_{o(10:1)} = i_{o(1:1)} \times \frac{0.1^{0.5} \times 0.9^{0.5}}{0.5^{0.5} \times 0.5^{0.5}} = 0.6\ i_{o(1:1)}$$

This will be true independent of the total concentration, as long as this remains constant. If, on the other hand, the redox ratio is kept constant, and the concentration changes, the exchange current should change proportionally to the total concentration change.

In a set of 1:10 to 10:1 redox ratios and 1 to 3Mtotal concentrations, as those investigated in this work, the exchange current will change most (under the present assumption) when changing from 1M (10:1), or 1M (1:10) to 3M (1:1). This maximum change in exchange current will be given by:

$$i_{o(3,1:1)} = i_{o(10:1)} \times \frac{(1.5)^{0.5} \times (1.5)^{0.5}}{(0.1)^{0.5} \times (0.9)^{0.5}} = 5\ i_{o(1,10:1)}$$

If we assume, on the other hand, an asymmetrical situation, such as $\alpha = 1 - \beta = 0.3$,

$$i_{o(1:10)} = i_{o(1:1)} \times \frac{0.1^{0.3} \times 0.9^{0.7}}{0.5} \simeq 0.9\ i_{o(1:1)}$$

$$i_{o(10:1)} = i_{o(1:1)} \times \frac{0.9^{0.3} \times 0.1^{0.7}}{0.5} \simeq 0.4\ i_{o(1:1)}$$

As before, this is independent of total concentration as long as it remains constant. In the same set of concentrations and ratios, as before the maximum variation will be obtained when changing from 3M (1:10) to 1M (10:1) as follows:

$$i_{o(3,1:10)} = i_{o(1,10:1)} \times \frac{0.3^{0.3} \times 2.7^{0.7}}{0.9^{0.3} \times 0.1^{0.7}} = 7.2\ i_{o(1,10.1)}$$